Abstract

LEE, HYUN JIK. Novel Cellulose Solvent System and Dry Jet Wet Spinning of Cellulose/ED/KSCN Solutions. (Under the direction of Dr. Richard Kotek).

The ethylenediamine/potassium thiocyanate salt (ED/KSCN) system was found to be a novel solvent system for the dissolution of cellulose. The solubility of KSCN in ED, the dissolution of cellulose, proper coagulants and coagulation rate of cellulose/ED/KSCN solution, dry jet wet spinning process of cellulose/ED/KSCN (7/65/35, w/w) solution and physical properties of cellulose fibers via the ED/KSCN solvent system were investigated. The maximum solubility of KSCN in ED was 44 wt% at room temperature and the ED/KSCN solvent had the best dissolving power on cellulose in ratio of ED/KSCN 65/35 (w/w). The dissolution of cellulose took place at a high temperature (60-70 ºC), and the maximum solubility was achieved 12 wt% for cellulose of DP 450 in the ED/KSCN 65/35 (w/w). Several different coagulants were tested for coagulation study and methanol was found to be a proper coagulant for our solvent system. Coagulation rate of methanol in the cellulose/ED/KSCN (7/65/35) solution was also calculated as 3.75×10^{-1} mm/min$^{1/2}$.

Cellulose fibers via the ED/KSCN solvent system were successfully produced by the dry jet wet spinning system. Cellulose fibers showed excellent mechanical properties compared to commercialized cellulose fibers such as Lyocell and rayon fibers. In our spinning system, spin draw ratio affected the mechanical properties of fibers the most. As the spin draw ratio increased, the fiber tenacity and fiber modulus tended to increase gradually, but fiber elongation decreased. For the morphology of cellulose fibers via the ED/KSCN solvent system, the fiber showed a round shape and a relatively compact structure, and micro-fibrils were not observed.

Novel Cellulose Solvent System and

Dry Jet Wet Spinning of Cellulose/ED/KSCN Solutions

by

Hyun Jik Lee

A thesis submitted to the Graduate Faculty of
North Carolina State University
in partial fulfillment of
requirements for the Degree of

Master of Science

Textile Technology & Management

Raleigh, North Carolina

2007

Approved by

Martin W. King	Xiangwu Zhang
Co-Chair of Advisory Committee	Member of Advisory Committee

Richard Kotek

Chair of Advisory Committee

BIOGRAPHY

Hyun Jik Lee was born on August 2nd, 1977, in Daegu, South Korea as a son of Young Mo Lee and Young Sook Song. He graduated from Kyung-sin High School in February 1996. He studied Textile Engineering in Yeoung-Nam University, South Korea from spring of 1996. After he spent one year in the university, he worked in the textile industry for two and half years. After experiencing the industry, he returned to the university and spent another one year. While studying for double majors with textiles and business in the school, his advisor suggested studying abroad for textile management. He prepared and transferred to the North Carolina State University in fall of 2002. He studied textile management for two and half years in NCSU then, graduated from NCSU with a Bachelor of Science degree in Textile Management in December in 2004.

After receiving the degree of Bachelor, he joined the graduate program in College of Textile in North Carolina State University in fall of 2005. And he studied for MS degree under Dr. Richard Kotek.

ACKNOWLEDGEMENTS

The author wishes to recognize the help and support of many people who have assisted in the project. First, the author would like to express his most sincere appreciation to Dr. Richard Kotek, the chairman of the Advisory Committee, for all the support, encouragement, and guidance throughout this study. The author would also like to thank the other committee members, Dr. Martin King and Dr. Xiangwu Zhang.

The author would like to express special thanks to Dr. John A. Cuculo for his suggestions, advice and encouragement in this study. In addition, deepest thanks go to Dr. Samuel M. Hudson for his kind assistance and expertise in the diffusion coefficient study. A particular appreciation is extended to Dr. Margaret Frey and her student, Min Xiao at Cornell University for their cooperation in the project.

A special recognition goes to the National Textile Center for their financial support of this work.

A particular thank is extended to Dr. Mehdi Afshari for his constant support, encouragement and guidance for the spinning process.

Finally, the author wishes to express his gratitude to family members and friends in Korea.

TABLE OF CONTENTS

LIST OF TABLES ..... **vi**

LIST OF FIGURES ..... **viii**

CHAPTER 1. Introduction **1**

CHAPTER 2. Literature Review I – Cellulose Dissolving Techniques **3**

2.1 Introduction 3

2.2 N-Methylmorpholine N-Oxide And Water 6

2.3 N, N-Dimethylacetamide and Lithium Chloride 8

2.4 Ionic Liquids 10

2.5 Amonia/Amonium Thiocyanate 13

2.6 Amine-Salt 15

CHAPTER 3. Literature Review II – Dissolution Mechanism of Ethylenediamine/Salt Solvent System. **18**

3.1 Introduction 18

3.2 Dissolution of Cellulose in the ED/salt Solvent System 20

3.3 FTIR Analysis 22

3.4 ^{39}K and ^{14}N NMR Spectroscopy Analysis 26

3.5 X-ray Diffraction Analysis 29

CHAPTER 4. Literature Review III - N-Methylmorpholine-N-Oxide or Lyocell Process **32**

4.1 Introduction 32

4.2 Preparation of Cellulose-N-Methylmopholine-N-Oxide Solution 35

4.3 Fiber Formation and Properties of Lyocell Fibers 37

CHAPTER 5. Experimental Procedure **40**

5.1 Materials.. 40

5.2 Intrinsic Viscosity Measurement 40
5.3 Dissolution of Cellulose 41
5.3.1 ED/KSCN and ED/NaSCN Solvent Preparation 41
5.3.2 Cellulose/ED/KSCN Solution Preparation 42
5.4 Coagulation Study 43
5.4.1 Film Formation 43
5.4.2 Measurement of Coagulation Rate of Cellulose Solutions 44
5.5 Dry Jet-Wet Spinning of Cellulose/ED/KSCN Solution 45
5.6 Characterization of Cellulose Fibers via ED/KSCN Solvent System 47
5.6.1 Tensile Properties of Cellulose Fibers 47
5.6.2 X-ray Diffraction Analysis 47
5.6.3 FTIR Spectroscopy Analysis 47
5.6.4 DSC Analysis 48
CHAPTER 6. Results and Discussion 49
6.1 Viscosity Measurement 49
6.2 Solubility of Cellulose in the ED/KSCN and ED/NaSCN Solvent 55
6.3 Coagulation Studies 58
6.3.1 Film Formation 58
6.3.2 Coagulation and Boundary Movement 62
6.3.3 Diffusion Coefficient 65
6.4. Dry Jet-Wet Spinning of the Cellulose/ED/KSCN Solutions 68
6.5 Characterization of Cellulose Fibers via ED/KSCN Solvent System 71
6.5.1 Mechanical Properties of Cellulose Fibers via ED/KSCN Solvent 71
6.5.2 Scanning Electron Microscopy (SEM) Analysis 73
6.5.3 FTIR and DSC Analysis of Cellulose Fibers 75
CHAPTER 7. Conclusion 78
CHAPTER 8. Future Work 80
References…. 82

LIST OF TABLES

Table 2.1 Dissolution of Cellulose Pulp (DP ≈ 1000) in Ionic Liquid [6] 11
Table 2.2 Dissolving Power for Cellulose (DP 210) in the Amine/Salt Solvent System [46] 16
Table 2.3 Mechanical Properties of Cellulose Fibers (DP 210) Spun from the Ethylenediamine/NaSCN System [46] 17
Table 3.1 Changes in Absorption Band of Cellulose before and after Precipitating [21] 25
Table 3.2 Changes in X-ray Diffraction Angles of Cellulose Before and After Precipitation [21] 31
Table 4.1 Effect of Various Factors on Cellulose Dissolution in NMMO-Water [6] 36
Table 4.2 Lyocell Process Variables [6] 38
Table 4.3 Properties of Various Cellulose Fibers (0: Minimal, 6: Maximum degree of fibrillation) [41] 39
Table 6.1 Viscosity Measurement of AV Cellulose 51
Table 6.2 Viscosity Measurement of VFC Cellulose 52
Table 6.3 Intrinsic Viscosity of AV Cellulose and VFC Cellulose Calculated From Different Methods 52
Table 6.4 Molecular Weight and Degree of Polymerization (DP) of AV Cellulose and VFC Cellulose 53
Table 6.5 Solubility of VFC Cellulose (DP 450) in Different Ratio of ED/salt Solvents: X (No Solution), O (Solution), Δ (Partially Dissolved Solution) 56
Table 6.6 Solubility of KSCN in Different Coagulants 59
Table 6.7 Comparison of Coagulation Rate of Each Coagulant vs. Min. Coagulation Rate .. 64
Table 6.8 Experimental Values of Boundary Distance of Cellulose/ED/KSCN (7/65/35) Solution with Several Coagulants for 120 minutes 66
Table 6.9 Typical Spinning Conditions of the Dry Jet-Wet Spinning in the ED/KSCN Solvent System 70
Table 6.10 Mechanical Properties of Cellulose Fibers via ED/KSCN Solvent 72

Table 6.11 Mechanical Properties of Commercial Cellulose Fibers vs. Cellulose Fibers via ED/KSCN Solvent System 72

LIST OF FIGURES

Figure 1.1 Chemical Structure of Cellulose [1] 1
Figure 2.1 X-ray diffractograms of four cellulose polymorphs [5] 4
Figure 2.2 Transition Possibilities between the Various Types of Crystalline Cellulose [5] ... 5
Figure 2.3 Chemical Structure of N-mthylmorpholine-N-oxide (NMMO) [6] 6
Figure 2.4 Chemical Structure of N, N-dimethylacetamide [6] 8
Figure 2.5 Structure of 1-butyl-3methylimidaxolium chloride [6] 10
Figure 2.6 Chemical Structure of Hydrazine [6] 15
Figure 2.7 Chemical Structure of Ethylenediamine [6] 15
Figure 3.1 Polarized Light Microscopy Images of 3 wt% CC 41 Cellulose Dissolved in (a) ED/KSCN, (b) ED/KI, (c) ED/NaSCN and (d) ED/NaI [21] 21
Figure 3.2 FTIR spectra of; (a) Cellulose/ED/KSCN mixture, (b) Mixture after one temperature cycling, (c) Cellulose/ED/KSCN solution [22] 23
Figure 3.3 FTIR Spectra of Cellulose; (a) Pure CC41 Cellulose (DP 210), (b) CC41 Cellulose recovered from cellulose swollen in ED, (c) CC41 Cellulose recovered from cellulose/ED/KSCN (5/77/23) solution [21] 25
Figure 3.4 ^{39}K NMR Spectra of Cellobiose (DP 2) Solution in ED/KSCN (92.3/7.7, w/w) Solvent [21] 27
Figure 3.5 ^{14}N from KSCN NMR Spectra of Cellobiose Solution in ED/KSCN (92.3/7.7) Solvent [21] 27
Figure 3.6 ^{19}N from EDA NMR Spectra of Cellobiose Solution in ED/KSCN (92.3/7.7 w/w) Solvent [21] 28
Figure 3.7 X-ray Diffractograms for CC41 Cellulose: (A) Pure CC41 Cellulose, (B) CC41 Cellulose Recovered from Cellulose Swollen in ED, (C) CC41 Cellulose Recovered from a 5 wt% of Cellulose Solution with a ED/KSCN Solvent (77/23, w/w) [21] 31
Figure 4.1 Schematic of NMMO Process [6] 34

Figure 5.1 Experimental Set-up for Cellulose Dissolution Process 43
Figure 5.2 Schematic of Coagulation Rate Experiment Set-up 45
Figure 5.3 Schematic of the Dry Jet-Wet Spinning System of Cellulose Fibers 46
Figure 6.1 Viscosity Measurement of AV Cellulose 54
Figure 6.2 Viscosity Measurement of VFC Cellulose 54
Figure 6.3 Polarized Light Microscopy Images of 5 wt% VFC Cellulose Dissolved in (a) ED/KSCN (65/35), (b) ED/KSCN (85/15), (c) ED/NaSCN (60/40) 57
Figure 6.4 Films coagulated in: (a) Water, (b) Ethanol, (c) Methanol, (d) 2-propanol and (e) Acetone 60
Figure 6.5 SEM Images of Cellulose Films Coagulated in Water and Methanol: (a) cross section of cellulose film coagulated in water, (b) surface of the cellulose films coagulated in water, (c) cross section of cellulose film coagulated in methanol and (d) surface of cellulose film coagulated in methanol 61
Figure 6.6 Boundary Movement in the Coagulation Process of Cellulose/ED/KSCN (7/65/35) Solution 64
Figure 6.7 Dependence of coagulation rate at 120 min on the molecular volume of the coagulants for cellulose/ED/KSCN (7/65/35) 67
Figure 6.8 Viscosity of Cellulose/ED/KSCN (7/65/35) Solution at 60ºC 67
Figure 6.9 Viscosity Comparison for: a) Free Flowing Fiber Forming Cellulose/ED/KSCN (7/65/35) Solution b) Non-fiber Forming Highly Viscous Solution of Cellulose in 1-butyl-3-methylimidazolium chloride (ionic liquid). C = 7% w/w; DP = 450. 70
Figure 6.10 SEM Images of Cellulose Fibers Produced via ED/KSCN Solvent system: (a) Cross-section of cellulose fibers with cold drawing, (b) Cross-section of cellulose fibers with hot drawing, (c) Surface of cellulose fibers 74
Figure 6.11 FTIR Spectra of VFC Cellulose Pulp and Cellulose fibers spun by ED/KSCN Solvent System 76
Figure 6.12 DSC Thermogram of Cellulose/ED/KSCN (7/65/35) Solution and Cellulose Fibers via ED/KSCN Solvent system 77

CHAPTER 1. Introduction

Cellulose (Figure 1.1) is considered to be one of the most abundant natural polymers worldwide as well as a biodegradable and renewable polymer [1]. The most common sources of cellulose for industrial purpose are wood pulp and cotton lint. Highly purified wood pulp consists of 95 – 99% cellulose and is called such terms as ‘chemical cellulose’ and ‘dissolving pulp’ [2]. These chemical cellulose or dissolving pulps are utilized for manufacturing man-made fibers (e.g. viscose rayon, cellulose acetate), films (e.g. cellophane) and derivatives which may be used as plastics and for many other purposes [2].

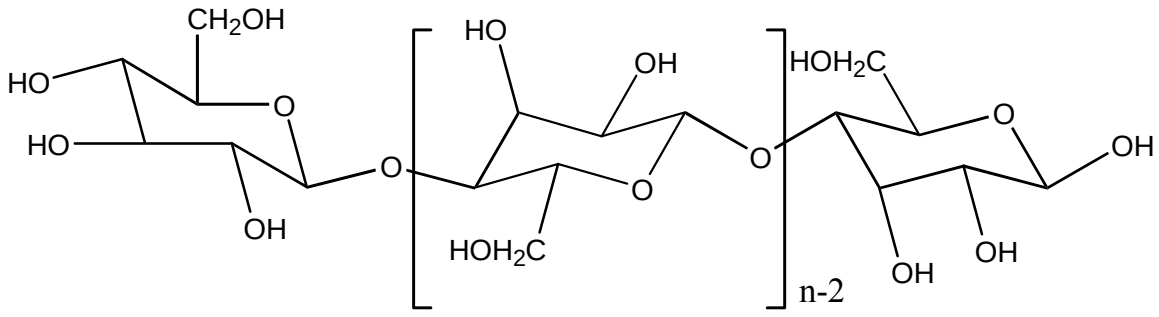

Figure 1.1 Chemical Structure of Cellulose [1]

Despite lots of advantages regarding end use of cellulose, there is undoubtedly a need for multiple solvents system and a large amount of time to achieve cellulose dissolution. In addition, by-products and side reaction in the cellulose dissolving process have significant negative environmental and health effects that are cost ineffective. A 20-year research and development cycle lead to cleaner process, called the Lyocell process, utilizing direct

dissolution of cellulose in n-methyl morpholine n-oxide. Although the Lyocell process produces excellent cellulose fibers and is commercially successful, it has not been able to replace rayon in all applications [3].

The objectives of this study are the dissolution of cellulose via our new solvent system and the formation of a family of cellulose fibers ranging in properties from conventional textile to high performance applications via the dry jet-wet spinning system. Cellulose fibers successfully spun by our new solvent system will be analyzed by Scanning Electron Microscopy (SEM), FTIR and DSC and compared to commercial cellulose fibers.

CHAPTER 2. Literature Review I – Cellulose Dissolving Techniques

2.1 Introduction

Cellulose dissolving techniques are very important to both existing and potential applications of cellulose. The viscose process, one of the well-known cellulose dissolving techniques, has long provided the framework for the rayon and cellulose film industries. The use of cellulose solvents is also one of the significances for characterizing cellulose materials. It would appear that expanded use of cellulose materials in the years ahead will depend heavily on the degree to which cellulose solvents can be economically exploited [2].

The dissolution of cellulose must recognize that cellulose can exist in four types of polymorphic forms, cellulose I, II, III, and IV, which are easily distinguished by X-ray diffraction [4-5] (Figure 2.1).

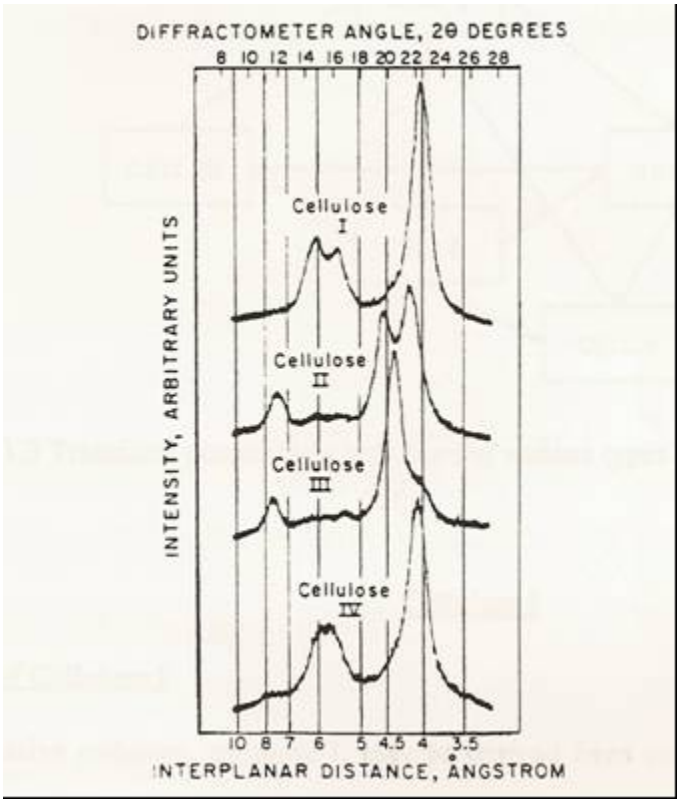

Figure 2.1 X-ray diffractograms of four cellulose polymorphs [5]

Cellulose I is the crystal form of native cellulose. Cellulose II is typically produced from regenerated cellulose or mercerized cellulose. Cellulose III is generated by pretreatment of cellulose with liquid ammonia (NH_3) or organic amines (RNH_2) followed by their anhydrous removal. Cellulose IV is prepared by heat treatment of cellulose with glycerol ($CH_2(OH)CH(OH)CH_2(OH)$). Transformations among cellulose polymorphs are possible [4-5] (Figure 2.2). It is important to understand these distinctions because the respective cellulose polymorphs can have different solubility characteristics in particular solvents.

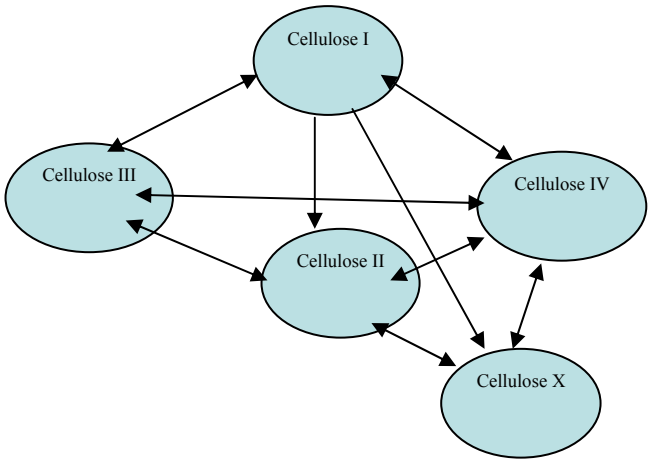

Figure 2.2 Transition Possibilities between the Various Types of Crystalline Cellulose [5]

Textile research and development activities devoted to new cellulose solvents worldwide have been especially prolific over several years and have introduced many new cellulose solvent systems. The main goal of this literature review is to present several examples of cellulose solvents that illustrate the variety of different solvent systems that exist, focus on what is known about their chemistry, and indicate potential applications of these systems for commercial processing of cellulose or cellulose derivatives.

2.2 N-Methylmorpholine N-Oxide And Water

The dissolution of cellulose in the N-methylmorpholine-N-oxide (NMMO, Figure 2.3) solvent system is one of the cellulose solvent systems which is developed and commercialized recently by Courtaulds. Ideally, dissolution of cellulose in the NMMO is supposed to be an entirely physical process without any chemical changes being caused in the pulp or in the solvent. However, even though NMMO solvent system has the convenient property of being cellulose solvent, it is a strong oxidant, solid at room temperature (which requires high temperatures to produce a tractable spinning dope) and a rather unstable compound. Therefore, in real-world processes, the NMMO solvent system requires numerous chemical process, which are strongly interrelated and rather complex [7-10].

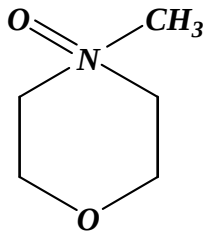

Figure 2.3 Chemical Structure of N-mthylmorpholine-N-oxide (NMMO) [6]

The preparation of the cellulose solutions with NMMO solvent system includes adding cellulose to a mixture of aqueous NMMO and n-propyl gallate (PG). The PG, the most widely applied NMMO stabilizer nowadays, is specially used as a phenolic antioxidant to stabilize the degree of polymerization (DP) of the cellulose and is finally oxidized to a deeply colored, highly conjugated chromophore. The mixture is placed in an airtight vessel

and then stirred and heated at 130ºC [6]. Much care is required in heating the mixture of compounds because temperature above 150ºC can cause rapid decomposition of the solvent and lead to explosions. Complete dissolution of cellulose normally takes place within 30 min at 130ºC and is even faster under optimum conditions [6, 11-12].

The chemical reactions in NMMO solvent system also have several negative effects: increased consumption of NMMO, increased degradation of cellulose (DP loss) with resulting decreased product performance, increased formation of degradation products, which must be removed from the system, increased chromophore formation, and decreased chemical stability of the system, even leading to blasts and an explosion. Especially, the chromophore formation causes a number of secondary, undesired side effects, such as temporary or permanent discoloration of the resulting fibers, a reduced bleachability of the fiber material, and a high load of dark colored compounds in the spinning dope, which must be continuously removed [12].

The NMMO solvent system, however, is still particular interesting because it can dissolve very high concentration (up to 50%) of cellulose and lead to the formation of anisotropic solutions [6].

2.3 N, N-Dimethylacetamide and Lithium Chloride

N, N-dimethylacetamide (Figure 2.4) and lithium chloride solvent system was first discovered to dissolve polyamides and chitin in 1972. This solvent system rapidly spread and the application for dissolution of cellulose was done for the first time by McCormick and Turbak [14]. This solvent system became very common in cellulose chemistry. The mixture of this solvent can achieve dissolution of cellulose within a certain concentration range of LiCl and cellulose. It is widely used for analytical purpose, such as in GPC (gel permeation chromatography) measurements, and also in organic synthesis, such as for homogeneous derivatization reactions [6, 13]. The clear advantage of LiCl/DMAc solvent system is directly linked to derivatization with being faster, easier and more reproducible [14].

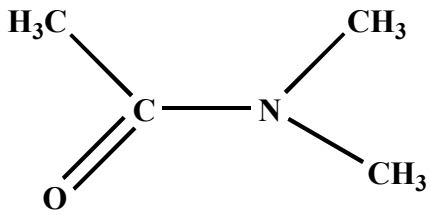

Figure 2.4 Chemical Structure of N, N-dimethylacetamide [6]

The mechanism of dissolution of cellulose in this solvent is believed to proceed through the formation of complexes between the solvent and the cellulosic hydroxyl groups [6]. Both LiCl and DMAc are very hygroscopic, and so water has to be excluded from LiCl/DMAc solvent system, since its presence prevents complexation with cellulose and accelerates the formation of polymer aggregates. The procedure for dissolving cellulose with this solvent involves prewetting the cellulose with DMAc. A known weight of DMAc is

combined with a certain amount of dried cellulose. The mixture of DMAc and dried cellulose is distillated at approximately 165ºC in a nitrogen atmosphere for 20-30 min. The mixture is cooled down to about 100ºC and a predetermined amount of LiCl is added while stirring. Continued stirring at 80ºC for 10-40 min guarantees complete dissolution of cellulose. Typically, complete dissolution of cellulose with LiCl/DMAc solvent system containing 10% lithum chloride can be achieved with cellulose concentration up to 15% (w/w) (DP = 130) but at higher DP (~ 1700), concentrations are limited to about 4% (w/w). Above the certain critical cellulose concentration, depending on the DP of cellulose, undissolved and swollen particles of cellulose are observed in the viscose solutions [2, 6, 13-14].

The solutions of cellulose in LiCl/DMAc solvent system are extremely stable. Some scientists found that no degradation of the cellulose occurred in the solution after several months and even years at room temperature. High concentrations of LiCl above 10% were reported to protect degradation effects on cellulose over time. A slight decrease of 2% in relative viscosity of cellulose solutions can be observed in 9% LiCl/DMAc over 30 days. They attribute to changes in inter- and intra-molecular hydrogen bonding in cellulose [14].

2.4 Ionic Liquids

Ionic liquids indicate a group of new salts that exist as liquids at a relatively low temperature, less than 100ºC. This solvent shows many attractive properties; for example, chemical and thermal stability, non-flammability and immeasurable low vapor pressure (even up to 300ºC). Unlike traditional unstable organic compounds and because of these advantages, ionic liquids are called “green” solvents and have been used widely as reaction media. As a result, they have received a lot of attention [15].

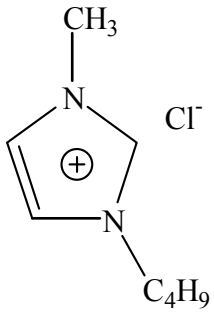

Figure 2.5 Structure of 1-butyl-3 methylimidazolium chloride [6]

As early as 1934, Graenacher discovered that molten N-ethylpyridinium chloride, in the presence of nitrogen containing bases, could be used to dissolve cellulose. This might be the first experience of cellulose dissolution using ionic liquids [15]. Huddleston et al., then, studied a series of hydrophilic and hydrophobic 1-alkyl-3methylimidazolium ionic liquids. Based on these investigations, Roger and his coworkers have shown that cellulose can possibly be dissolved in some hydrophilic ionic liquids, for example 1-butyl-3-

methylimidazolium chloride (BMIMCI) (Figure 2.5) and 1-allyl-3-methylimidazolium chloride (AMICMI) (Table 2.1) [6, 15].

Table 2.1 Dissolution of Cellulose Pulp (DP ≈ 1000) in Ionic Liquid [6]

Ionic Liquid	Method	Solubility (wt %)
$[C_4min]Cl$	Heat (100ºC)	10
$[C_4min]Cl$	Heat (80ºC) + sonication	5
$[C_4min]Cl$	Microwave heating 3-5 pulses	25 (clear viscose solution)
$[C_4min]Br$	Microwave	5-7
$[C_4min]SCN$	Microwave	5-7
$[C_4min][BF_4]$	Microwave	Insoluble
$[C_4min][PF_6]$	Microwave	Insoluble
$[C_4min]Cl$	Heat (100ºC)	5
$[C_4min]Cl$	Heat (100ºC)	Slightly soluble

Cellulose, whether it is refined or natural, can be dissolved without any derivation in some hydrophilic ionic liquids. Solubility of cellulose and its solution properties can be easily controlled by the selection of the ionic liquid compounds. As shown at Table 2.1, microwave heating can significantly increase its solubility. Solutions including up to 25 wt% cellulose can be prepared in BMIMIC under microwave heating. The high chloride concentration and activity in BMIMIC is assumed to be highly effective in breaking the extensive hydrogen-bonding network present in cellulose and is the key factor in this dissolution process [6, 15].

Cellulose in its BMIMCI solution can be easily precipitated by the addition of water, ethanol or methanol. The regenerated cellulose is hardly degraded and has almost the same degree of polymerization and polydispersity as the initial cellulose. Its morphology however, significantly changes and its microfibrils are fused into a relatively homogeneous

macrostructure. By changing the regeneration processes, the regenerated cellulose can be in a range of structural forms, such as powder, tube, beard, fiber and film [15]. The ionic liquids can be recovered and reused by various methods, such as evaporation, ionic exchange, reverse osmosis and salting out [15].

2.5 Amonia/Amonium Thiocyanate

In 1980, Cuculo and Hudson discovered that ammonia/ammonium thiocyanate (NH_3/NH_4SCN) has an excellent dissolving power as a solvent for cellulose. Their studies have shown that true cellulose solutions are achieved in this solvent system. They developed the relationship of viscosity and molecular weight and revealed maximum solubility of a dissolving pulp (concentration up to 14 % w/w) in the solvent system. In addition, the solutions have been shown to exhibit thermoreversible gelation, and fiber formation has been demonstrated. They also reported that the solvent has several practical advantages, including low production cost and readily available components [2, 6].

The boiling point of the solvent is relatively low (~ 70ºC) when compared to other solvents; as a result, it can be easily handled. There is no degradation of cellulose and there seems to be no reaction between the cellulose and the solvent [16, 17]. Solvent preparation (NH_3/NH_4SCN 24.5/75.5) is very simple. NH_4SCN is dried and purified by recrystallization from NH_3 and then dried. The NH_3/NH_4SCN is prepared by deliquescing NH_3 on a known amount of dried and purified NH_4SCN to obtain a composition of 24.5/75.5 w/w [5]. Dissolution of the salt, then, occurs easily and the solvent is ready to use.

While researching on these solvent studies, a novel and powerful dissolution method was invented for the rapid and convenient dissolution of cellulose. This technique is called rapid temperature cycling by the authors. This dissolution technique has been used remarkably well in the laboratory. The rapid temperature cycling technique is performed as follows [6].

1. Respective known weights of cellulose and NH_3/NH_4SCN solvent are placed in the sealable polyethylene bag.

2. These mixed compounds are homogenized with hand mixing.

3. The polyethylene bag is then subjected to the temperature cycling process, which includes placing the bag in a cold bath (-33ºC) for a few minutes.

4. The mixture is subject to shearing forces by passing the bag forward and backward through a rolling pin at room temperature.

5. The bag is then placed at higher temperature (40ºC).

6. The mixture is subjected several times to this temperature cycling process for the complete dissolution of cellulose.

Over the years, the NH_3/NH_4SCN solvent system, especially determined the intimate mechanism of dissolution of cellulose in the solvent and has been extensively researched by many textile scientists. They revealed that the temperature cycling sequences in this dissolution technique break specific cellulose inter- and intramolecular hydrogen bonds, and cellulose is transformed from polymorph I to II to III to IV and finally to amorphous as dissolution proceeds [6, 18].

2.6 Amine-Salt

Hattori et al. have recently reported a two component system (amine-salt) consisting of hydrazine (NH_2-NH_2) (Figure 2.6) or ethylenediamine (NH_2-CH_2-CH_2-NH_2, ED) (Figure 2.7) and various thiocyanate salts such as LiSCN, NaSCN, or KSCN that can effectively dissolve cellulose pulp [6]. However, this solvent system requires high concentration of salt (40-50%) to obtain high concentration cellulose solutions (up to 18-20% w/w). The researches working on this study have shown that cellulose I, II, and III can be effectively dissolved in an amine-salt solvent [6].

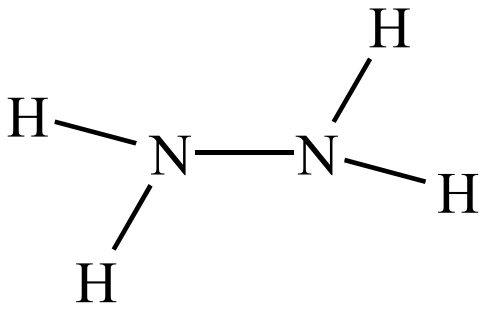

Figure 2.6 Chemical Structure of Hydrazine [6]

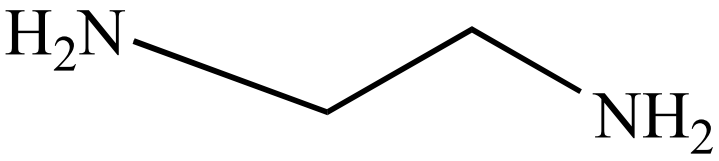

Figure 2.7 Chemical Structure of Ethylenediamine [6]

The most remarkable point of the amine-salt dissolution process developed by Cuculo and Hattori is the temperature cycling step. Although, cellulose is not required to undergo pre-activation in the dissolution process, temperature cycling must be used to dissolve the cellulose pulp. Generally, dissolution process does not take place if the cellulose is just placed in an amine-salt solvent. In a typical temperature cycling procedure, cellulose pulp is combined with a thiocyanate salt and amine (hydrazine or ethylenedimine) solvent in a sealable polyethylene bag in presence of nitrogen. The mixture is then cooled down to -10ºC for about an hour and then warmed up to 50ºC with intermittent shearing for 30 min [6]. The temperature cycling step is required several times for the complete dissolution of cellulose pulp. Studies have shown that cellulose (DP 210) solution with concentration of 18% w/w can be easily prepared by using this technique (Hattori's Presentation). Hattori also reported that the mixture of hydrazine or ethylenedimine and NaSCN as cellulose solvent has the most dissolving power among other mixtures (Table 2.2).

Table 2.2 Dissolving Power for Cellulose (DP 210) in the Amine/Salt Solvent System [46]

Solvent System	Salt Solubility (g/100g of amine)	Dissolving Power (% (w/w))
NH_3/NH_4SCN	399	27
NH_2NH_2/NaSCN	91	18
NH_2NH_2/KSCN	200	14
NH_2NH_2/NaI	66	16
$NH_2CH_2CH_2NH_2$/NaSCN	86	18
$NH_2CH_2CH_2NH_2$/KSCN	81	14
$NH_2CH_2CH_2NH_2/Ca(SCN)_2$	Insoluble	Insoluble

The author suggested that the amine-salt solvent system based on ethylenedimine rather than hydrazine has greater potential for the fiber and film formation of regenerated cellulose [6]. Cellulose fibers spun from the Ethylenediamine/NaSCN solvent system are successfully produced and show great mechanical properties (Table 2.3). Frey et al. have also shown that a cellulose solution via the amine-salt solvent can be converted into nanofibers by using the electro-spinning process. Thus, so far these recent, positive achievements indicate that this amine-salt solvent system can be further developed for producing commercial cellulose fibers and used for environmentally friendly cellulose solvent.

Table 2.3 Mechanical Properties of Cellulose Fibers (DP 210) Spun from the Ethylenediamine/NaSCN System [46]

Cellulose Concentration (% (w/w))	Tenacity (g/denier)	Modulus (g/denier)
8	2.9	160
10	3.2	172
12	4.2	186
Cf. Tencel®	5.8	205

CHAPTER 3. Literature Review II – Dissolution Mechanism of Ethylenediamine/Salt Solvent System.

3.1 Introduction

Hudson and Cuculo et al. have been studying the dissolution of cellulose in ammonia/ammonium thiocyanate and analogous solvent system including hydrazine/salt and ethylenediamine/salt. Three different solvents have been found to be able to dissolve cellulose successfully. However, hydrazine/salt solvent is relatively toxic and carcinogenic, which makes it a poor alternative. The ethylenediamine/salt solvent is less volatile than the ammonia/ammonium solvent and easily swells cellulose and facilitates the diffusion to the tightly packed crystalline regions of cellulose [20]. These advantages of the ED/salt solvent system show good potential to be utilized with cellulose, which can be possibly developed to the commercial level.

Cuculo et al. determined that the temperature cycling technique in the dissolution of cellulose in the ethylenediamine/salt solvent system efficiently disrupted hydrogen bonding between and within cellulose chains. Successive temperature cycling between -40ºC and 30ºC transformed cellulose structure from cellulose I crystal formation to II to III, then to amorphous. Once the cellulose structure turned to amorphous, dissolution of cellulose in the solvent system took place [19].

This chapter presents a review of the dissolution mechanism of cellulose in the ethylenediamine/salt solvent system including the role of salt on cellulose dissolution in this solvent system. Changes in interactions between cellulose and ethylenediamine are analyzed

via changes in the FTIR spectra. ^{39}K and ^{14}N NMR analysis is used to find out how salt affects the dissolution process of cellulose. Finally, wide angle X-ray diffraction studies are also used to analyze how the ED/KSCN solvent effectively diffuses into the cellulose crystalline region and breaks the hydrogen bonding in cellulose.

3.2 Dissolution of Cellulose in the ED/salt Solvent System

Cellulose displays different behavior in the different ED/salt solvent systems. Figure 3.1 shows the images of 3 wt% of CC41 cellulose (DP 210) in different ED/salt solvent systems under a polarized light microscope. The different ED/salt solvents are made of the ratio of 89/11 (mol/mol) ED/salt. The image of cellulose solution in ED/KSCN looks completely dark in Figure 3.1 (a), indicating the complete dissolution of cellulose. The cellulose solution in ED/KI (Figure 3.1 (b) is almost dissolved but some undissolved cellulose particles are observed. However, the images of the cellulose solutions in ED/NaSCN and ED/KI (Figure 3.1 (c), (d)) show a large amount of undissolved cellulose fibers which indicate the poor dissolving power of NaSCN and NI for cellulose under the selected solvent system [21].

According to the different salt tests in the ED/salt solvent system, KSCN has the best dissolving power and can dissolve a wide range of molecular weights of cellulose in certain solvent concentration ranges.

Hattori et al. reported that maximum solubility achieved is 16% (w/w) for cellulose of DP 210 in ED/NaSCN 54/46 (w/w). Bacterial cellulose and some pulps are also dissolved in the solvent system. The cellulose solutions are stable for 30 days storage at room temperature and show mesophase formation of cellulose. Outside of the solvent composition, cellulose however has low solubility in ED/NaSCN [46].

(a) ED/KSCN

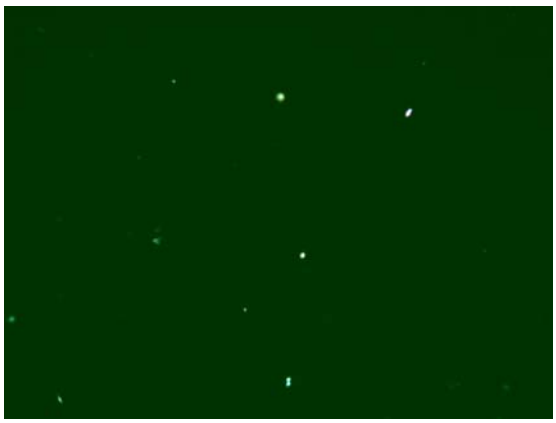

(b) ED/KI

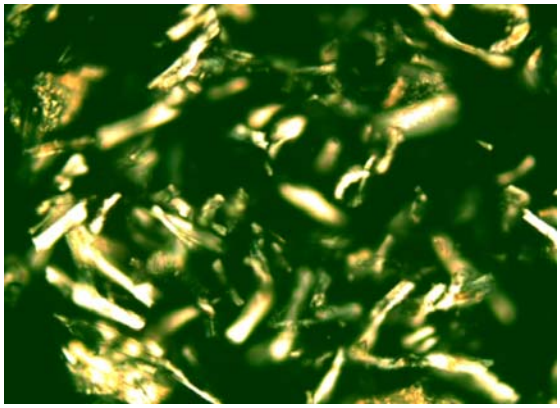

(c) ED/NaSCN

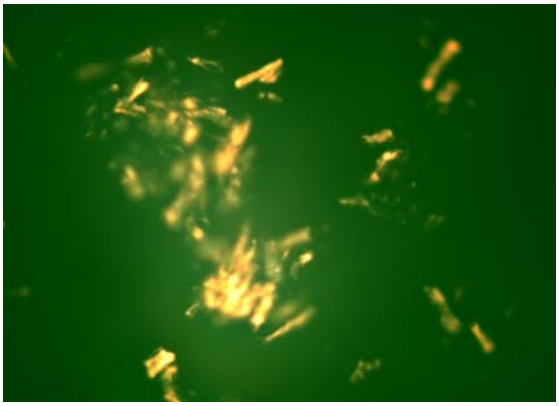

(d) ED/NaI

Figure 3.1 Polarized Light Microscopy Images of 3 wt% CC 41 Cellulose Dissolved in (a) ED/KSCN, (b) ED/KI, (c) ED/NaSCN and (d) ED/NaI [21]

3.3 FTIR Analysis

FTIR spectra (Figure 3.2) indicate the change in interaction between cellulose, ED, KSCN while the dissolution of cellulose takes place via temperature cycling. Spectrum (a) shows a mixture of cellulose, ED and KSCN, spectrum (b) shows a same mixture after 1 temperature cycling between -20 and 30ºC and spectrum (c) shows a solution of cellulose in ED/KSCN solvent. Hydrogen bonding, indicating an interaction between cellulose and EDA, display in hydrogen bonded N-H a stretching peak at 3200 cm^{-1} and the hydrogen bonded C-H a stretching peak at 2750 – 2700 cm^{-1}. Several split peaks below 2000 cm^{-1} in the Figure 3.2 (a) are changed gradually to single band as the system progresses from a mixture of dissolved and undissolved cellulose to homogenous solution. However, the sharp peak at 2700 cm^{-1}, indicating the characteristic of the SCN^- anion, is not affected during the dissolution process [22].

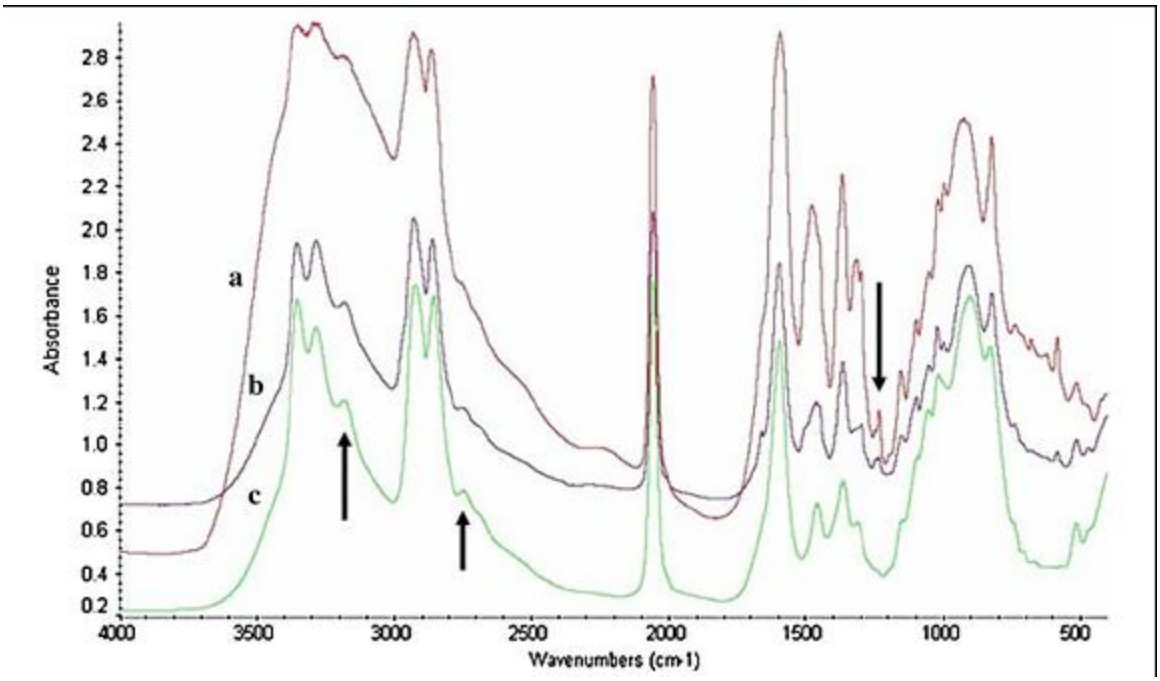

Figure 3.2 FTIR spectra of; (a) Cellulose/ED/KSCN mixture, (b) Mixture after one temperature cycling, (c) Cellulose/ED/KSCN solution [22]

Previous studies have reported that alkali metal cations such as K^+ can form complexes with cellulosic materials [23]. Like other cellulose solvents work with different cations such as NH_4^+ in the NH_3/NH_4SCN solvent system and/or Ca^{+2} in the $H_2O/Ca(SCN)_2$ solvent system, in the ED/KSCN solvent system, co-ordination between the K^+ cation and cellulose appears to be critical to the dissolution of cellulose [22].

FTIR analysis is also used to determine changes in the conformation of cellulose chains and the crystal structure of cellulose swollen in ethylendiamine and the crystal structure of cellulose recovered from solution in ED/KSCN solvent. Figure 3.3 displays the FTIR spectra for pure CC41 cellulose, CC41 cellulose recovered by precipitating cellulose swollen in ED with water, and CC41 cellulose recovered by precipitating a

cellulose/ED/KSCN (5/77/23) solution with water. Table 3.1 lists the changes in the wavenumber (cm^{-1}) of the absorption bands of cellulose before and after precipitation in water. The absorption peak at 2900 cm^{-1} indicates a CH stretching vibration. As the dissolution of cellulose progresses from swelling in ED to solvation in the ED/KSCN solvent, the CH stretching frequency decreases from 2900 cm^{-1} to 2898 cm^{-1} to 2891 cm^{-1}. This phenomenon indicates that cellulose chains have undergone changes in intra- and/or inter-hydrogen bonding [21].

CH_2 symmetric bending and CH_2 wagging are, respectively, displayed by the absorption bands at 1,430 cm^{-1} and 1,317 cm^{-1}. Changes in the intensities and/or positions of these two bands indicate variations in the environment/conformation of the C-6CH_2OH group [24]. The intensity of the antisymmetric bridge oxygen stretching band at 1,163 cm^{-1} is decreased to 1161 cm^{-1} after recovering CC41 cellulose from the cellulose/ED/KSCN (5/77/23) solution. This indicates a change in the hydrogen-bonding of the bridge oxygen after the addition of salt in the system. The band at 894 cm^{-1}, assigned as C-O-C stretching of the β-(1 → 4)-glycosidic linkage, shows the characteristic of β-anomers or β-linked glucose polymers. The change in intensity of this band results from participation of the oxygen atom attached to C1 in this vibration and changes in the hydrogen bonding in cellulose [25].

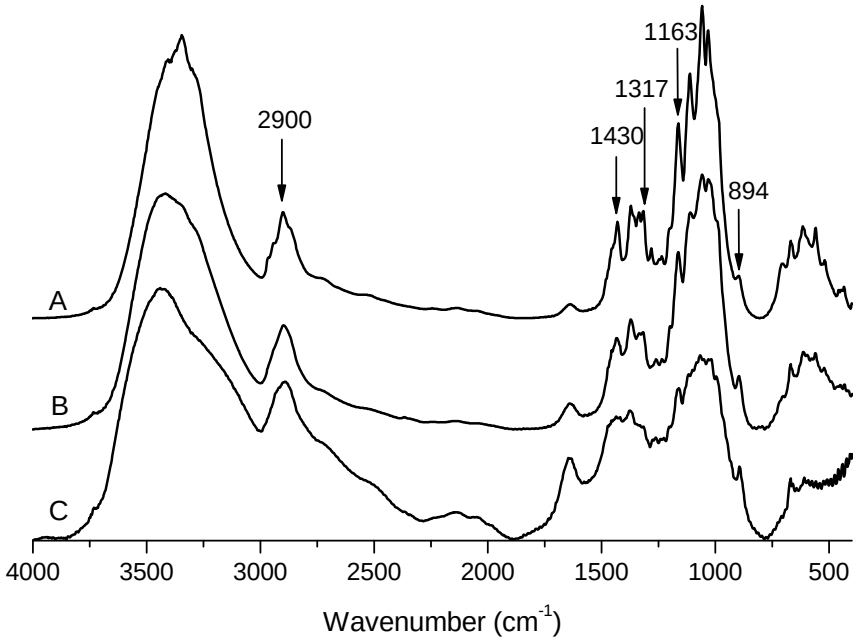

Figure 3.3 FTIR Spectra of Cellulose; (a) Pure CC41 Cellulose (DP 210), (b) CC41 Cellulose recovered from cellulose swollen in ED, (c) CC41 Cellulose recovered from cellulose/ED/KSCN (5/77/23) solution [21]

Table 3.1 Changes in Absorption Band of Cellulose before and after Precipitating [21]

Vibration Modes	Wavenumber (cm^{-1})		
	(a) Pure CC41	(b) CC41 Cellulose recovered from cellulose swollen in ED	(c) CC41 Cellulose recovered from cellulose/ED/KSCN (5/77/23) solution
CH stretching	2900	2898	2891
CH_2 symmetric bending	1430	1436	Weak
CH_2 wagging	1317	Weak	Weak
Antisymmetric bridge oxygen stretching	1163	1163	1161
C-O-C stretching	894	897	894

3.4 ^{39}K and ^{14}N NMR Spectroscopy Analysis

High resolution NMR spectroscopy is used to analyze how salt affects the dissolution of cellulose. For liquid-state NMR, the rapid tumbling of molecules in solution average out the molecular conformations and give rise to an average chemical shift [26]. That could be a reason why only a single peak is shown in the ^{39}K NMR spectrum, despite the fact that the K^+ ions exist in at least two chemically inequivalent environments (free and bound by cellobiose) [21]. In addition, molecular tumbling is reduced by increasing solution viscosity, therefore, as the concentration of solution increases, the spectra show broad the NMR signals and lower resolution [27].

Figure 3.4 – 3.6 displays ^{39}K and ^{14}N NMR spectra of cellobiose (DP 2) solutions in the ED/KSCN (92.3/7.7, w/w) solvent. 0 denotes no cellobiose in the solvent. The concentration of solution increases in the order of samples 1 to 5. Figure 3.4 shows that ^{39}K chemical gradually shifts to right side by increasing the concentration of solution. This appreciable shift of ^{39}K is explained by the increasing dominance of the peak associated with bound K^+ as more K^+ ions are moving toward cellobiose with increasing cellobiose concentration. On the other hand, no significant shift shows for N nuclei in Figure 3.5 and 3.6. This indicates that K^+ ion interacts with cellobiose more effectively than the SCN^- ion does [21].

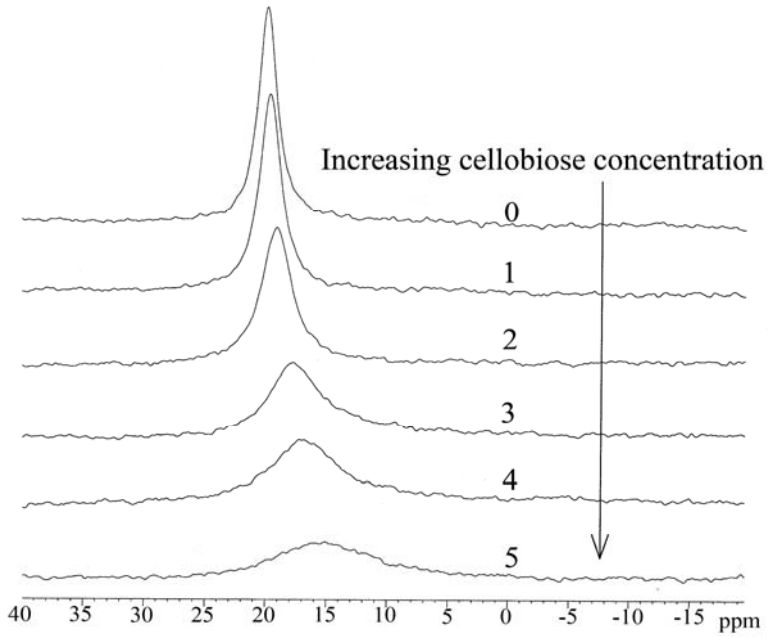

Figure 3.4 ^{39}K NMR Spectra of Cellobiose (DP 2) Solution in ED/KSCN (92.3/7.7, w/w) Solvent [21]

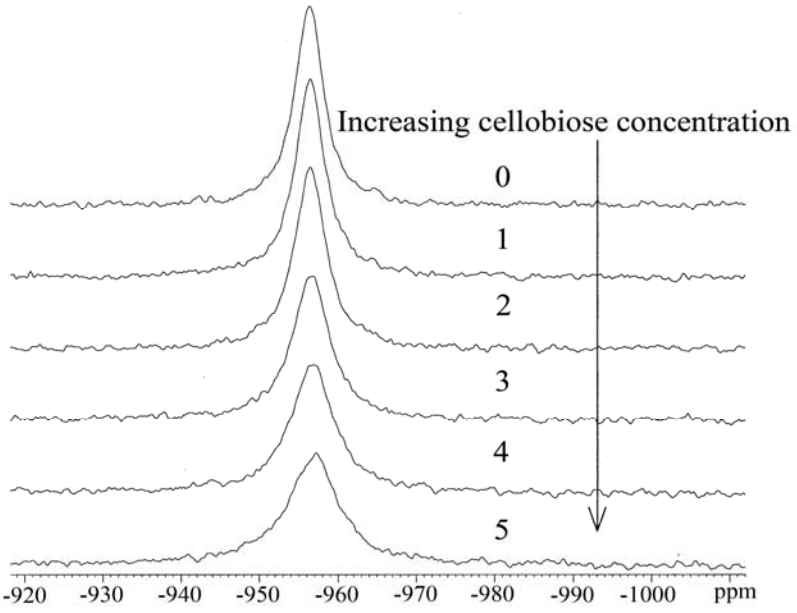

Figure 3.5 ^{14}N from KSCN NMR Spectra of Cellobiose Solution in ED/KSCN (92.3/7.7) Solvent [21]

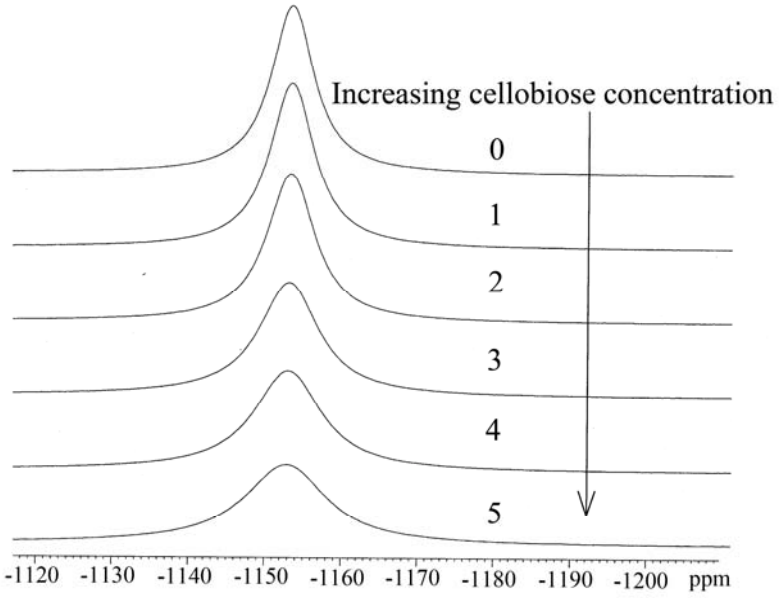

Figure 3.6 ^{19}N from EDA NMR Spectra of Cellobiose Solution in ED/KSCN (92.3/7.7 w/w) Solvent [21]

3.5 X-ray Diffraction Analysis

Changes in X-ray diffraction angles of cellulose before and after precipitation in water are investigated for cellulose polymorphs. Figure 3.7 shows the changes of X-ray diffraction angles, before and after precipitation of cellulose in water. Figure 3.7 (A), pure CC41 cellulose, displays three different diffraction angles at 2θ = 14.7, 16.4 and 22.6º. These values correspond to $(1\bar{1}0)$, (110) and (020) planes of cellulose I, respectively [28]. The recovered cellulose swollen in ED and precipitated in water shows a different polymorph. Two broad diffraction peaks are observed at 2θ = 16.2 and 22.0º (Figure 3.7 (B)). The recovered cellulose from the cellulose/ED/KSCN (5/77/23) solution exhibits diffraction angles at 2θ = 13.7, 20.1 and 21.7º (Figure 3.7 (C)). These diffraction angles are typical of cellulose II but, the peak at 13.7 is very broad and shows a slightly different point when compared to the published data, 2θ = 12.1º [28]. Table 3.2 shows organized values of diffraction angles from X-ray diffractograms in Figure 3.7.

Some studies reveal that intramolecular hydrogen bonds and intermolecular hydrogen bonds are shown in native crystalline cellulose, which is generally called cellulose I [29]. When native cellulose (cellulose I) swells in ED, cellulose I starts to form a complex with ED and has a different polymorph from cellulose I. A cellulose I-ED complex can, again, transform back to cellulose I when they are washed with water [30-31].

In this study, however, recovered cellulose which is swollen in ED and precipitated in water shows different results of polymorph from previous studies. The polymorph of those recovered cellulose assumes similar to the mixture of cellulose I and II. The recovered

cellulose from the CC41 cellulose/ED/KSCN (5/77/23) solution shows completely different polymorph from pure CC41 cellulose. The addition of KSCN causes recovered cellulose to convert from polymorph of cellulose I to II. This indicates that the CH_2OH group of cellulose for the crystalline component undergoes conversion from a t-g conformation for cellulose I to a g-t conformation for cellulose II. A g-t means that the C6-O6 bond is gauche to the C5-O5 bond and trans to the C4-C5 bond [32]. A new crystal structure in recovered cellulose has, then, developed with an intramolecular bond and an intermolecular bond [21].

A possible cellulose dissolution mechanism can be suggested from the combination of several analyses that the hydrogen bonding in cellulose is first weakened by adding ED molecules, then, KSCN is easily able to diffuse into the cellulose highly crystalline regions and interact with cellulose hydroxyl groups. This leads to the breaking of hydrogen bonding and development of new hydrogen bonds at new positions within the cellulose chains [21].

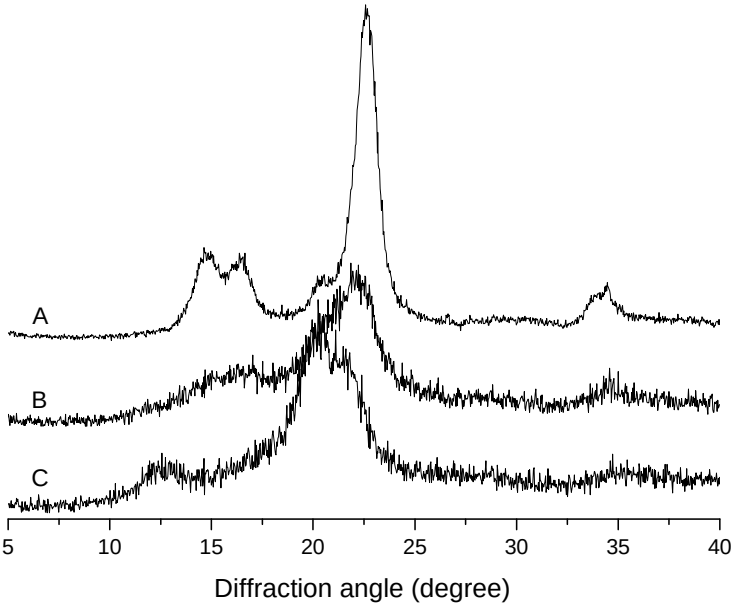

Figure 3.7 X-ray Diffractograms for CC41 Cellulose: (A) Pure CC41 Cellulose, (B) CC41 Cellulose Recovered from Cellulose Swollen in ED, (C) CC41 Cellulose Recovered from a 5 wt% of Cellulose Solution with a ED/KSCN Solvent (77/23, w/w) [21]

Table 3.2 Changes in X-ray Diffraction Angles of Cellulose Before and After Precipitation [21]

Regenerated Cellulose	X-ray Diffraction Angle (º)		
	$1\bar{1}0$	110	020
(a) Pure CC41 (DP 210, Cellulose I)	14.7	16.4	22.6
(b) CC41 Recovered from Cellulose Swollen in ED		16.2	22.0
(c) CC41 Recovered from a 5 wt% of Cellulose Solution (Cellulose II)	13.7	20.1	21.7

CHAPTER 4. Literature Review III - N-Methylmorpholine-N-Oxide or Lyocell Process

4.1 Introduction

Several solvent systems for the dissolution of cellulose were invented and introduced, but only three methods of processing cellulose into fibers were commercialized, such as the viscose rayon process, Bemberg™, and Lyocell (NMMO) process. The viscose rayon process was discovered in 1981 by the English chemist Charles Frederick Cross and his collaborators, Edward John Bevan and Clayton Beadle. It was commercialized 14 years later by the British company owned by Samuel Courtauld. The first commercialized rayon fibers were very successful. The fibers were accepted with enthusiasm by the textile trade, and Courtauld produced 150,000 lb annually. In 1910, the production was accelerated very rapidly, totaling 2,000,000 lb/year with the expansion of new equipments. As a result, viscose fibers became a viable human-made component of textile trade. In 1910, some American companies - DuPont, Tubize Company, Belamore – also opened their businesses to produce rayon [6].

However, there are some principal hazards in the viscose process, such as the exposures to carbon disulphide and hydrogen sulphide. Both have a variety of toxic effects depending on the intensity and duration of the exposure. They sometimes cause deep unconsciousness and death. Moreover, carbon disulphide has a high risk of fire and explosion with a flashpoint below -30ºC and explosive limits between 1.0 and 50%. There are also some other hazardous problems in the viscose process. The acids and alkalis used in the

process are fairly dilute, but there is always danger from preparing the proper dilutions and splashing into the eyes. The alkaline crumbs produced during the shedding process may irritate worker's hands and eyes, while the acid fumes and hydrogen sulphide gas emanating from the spinning bath may cause a kerato-conjunctivitis characterized by excessive lachrymation, photophobia and severe ocular pain.

Lyocell process or N-Methylmorpholine-N-Oxide (NMMO) process is a newly developed process for the production of cellulose fibers. Based on several studies of NMMO solvent system, Courtaulds succeeded to begin the commercial production of staple cellulose fibers, trademarked Tencel, in 1992. The Lyocell process is a modern, highly efficient, nonpolluting process when compared to the viscose rayon process. Fink et al. listed the following steps for the production of cellulose fibers [33]:

1. Preparation of a homogeneous solution (dope) from cellulose pulp in NMMO-water solution
2. Extrusion of the highly viscose spinning dope at elevated temperatures through an air gap into a coagulation bath (dry-jet wet-spinning process)
3. Coagulation of the cellulose fibers
4. Washing, drying, and post-treatment of the cellulose fibers
5. Recovery of NMMO from coagulation baths

As seen in Figure 4.1, Lyocell (NMMO) process is a closed loop process in which the NMMO can be recycled. The production cycle of Lyocell process is relatively short and does not exceed 8 hours [6]. On the other hand, the viscose rayon process is a very long process, exceeding more than 40 hours. The Lyocell fibers also have excellent mechanical properties,

but because of a high degree of crystallinity, the wet Lyocell fibers have increased susceptibility to fibrillation [6].

This chapter presents the review of more detailed studies of lyocell process from the preparation of cellulose NMMO solution to the properties of resulted fibers produced by Lyocell technique.

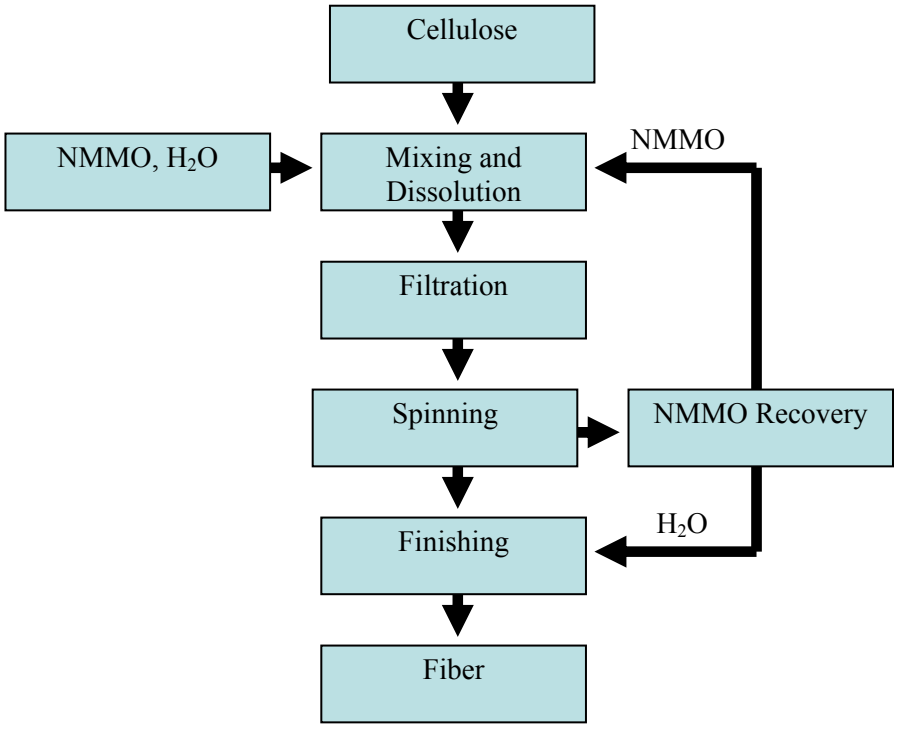

Figure 4.1 Schematic of NMMO Process [6]

4.2 Preparation of Cellulose-N-Methylmopholine-N-Oxide Solution

NMMO is the only organic solvent for the dissolution of cellulose which is commercially used for the production of cellulose fibers. The generic term "Lyocell" generally indicates the industrial process using NMMO solvent including the NMMO-cellulose mixture to the fiber production. NMMO or Lyocell process can normally produce highly concentrated spinning dope with cellulose concentration up to 35%, depending on the DP of cellulose, and has a rapid production cycle (less than 5 hours). Although NMMO process can prepare highly concentrated cellulose solution in a short time, there exist a few disadvantages. NMMO solvent includes an oxidizer, causing the degradation of cellulose, and is highly corrosive so that stainless steel equipments should be used for processing. At temperature higher than 150ºC in the process, NMMO can also cause undesired explosion by highly exothermic decomposition [34].

As raw materials for Lyocell fiber production, paper grade pulp, unbleached chemical pulp, cotton and rayon fiber wastes or even paper wastes can be used. In preparation of spinning dope, 50-60% of aqueous NMMO is used with the addition of 0.01-0.10% of antioxidant to prevent cellulose degradation. n-propyl gallate (PG) is typically used as an antioxidant. In a typical Lyocell industrial process, 50-60% NMMO, 20-30% water, and 10-15% cellulose pulp are used. Subsequently, water is efficiently evaporated at temperature lower than 150ºC and under reduced pressure until the cellulose solution is achieved [35]. According to several studies, the solubility of cellulose in the NMMO solvent is greatly affected depending on water content. In the dissolution process, one or two hydrogen bonds can be generally formed between the oxygen of N-O bond in NMMO and the hydroxyl group

of water, an alcohol, or cellulose [36]. At high water concentration, generally greater than 17 wt%, hydrogen bonds between NMMO and water dominate, thus preventing cellulose dissolution. In contrast, at low water concentration, less than 4 wt%, dissolution temperatures are very close to the decomposition point of NMMO and therefore, water concentration less than 4 wt% has the lower cellulose dissolution limit. At water concentration at about 10 wt%, the oxygen of the N-O bond in NMMO forms hydrogen bonds with hydroxyl groups of cellulose and dissolution can be achieved [37]. The effect of various process parameters on cellulose dissolution is shown in Table 4.1.

Table 4.1 Effect of Various Factors on Cellulose Dissolution in NMMO-Water [6]

Influencing Parameter		Solubility of Cellulose
Solution Temperature	Increased	Increased
Water Content of the Mixture	Increased	Decreased
Concentration of the Cellulose	Increased	Decreased
Molecular Weight of the Pulp	Increased	Decreased
Input of Mechanical Energy	Increased	Increased

4.3 Fiber Formation and Properties of Lyocell Fibers

Lyocell fibers are mostly produced by using a dry-jet wet spinning process for cellulose in an NMMO-water solution. The dry-jet wet spinning technique is relatively slow, with a spinning speed less than 100m/min when compared to other spinning systems. In this spinning system, coagulation is very important to determine the final speed of the process and the properties of resulting fibers. In commercial Lyocell process, water or NMMO solutions are generally used as coagulants. Air gap is another critical factor for the fiber formation in dry-jet wet spinning process. The polymer chain orientation takes place mainly in the air gap. Generally, a longer air gap leads to chain relaxation and a low degree of orientation [39]. The spinning temperature is also important for the Lyocell spinning process. The mechanical properties of Lyocell fibers normally decrease with increasing the spinning temperature. In general, if the spinning is performed at high temperature, an extrusion of solution increases and viscosity decrease. And if the spinning temperature is set above 130ºC, degradation of the cellulose and NMMO hydrate starts to occur, and it brings decreasing mechanical properties of fibers [40].

As mentioned above, the final properties of Lyocell fibers are determined depending on a number of variables. Table 4.2 shows possible variables in several conditions which can affect the properties of resulting fibers.

Table 4.2 Lyocell Process Variables [6]

Conditions	Variables
Spinning Dope Conditions	1. Polymer Concentration 2. Molecular Weight or Polydispersity 3. Additives (modifiers, stabilizers)
Spinning Conditions	1. Air Gap Length 2. Spinning Speed 3. Air Humidity 4. Draw Ratio 5. L/D for an Orifice
Coagulation Conditions	1. Coagulation Type 2. Composition of Coagulation Bath
Post-treatment Conditions	1. Drying Conditions 2. Post-treatment with Hot Water or NaOH Solution

Lyocell fibers are more crystalline and more oriented than viscose fibers. These characteristics lead to improved tensile properties for Lyocell fibers. Also, they have a oval or round shape in cross section of fibers and tend to be highly fibrillar. Lyocell fibers also show skin-core morphology, where the skin is denser than the core that can be obtained only if coagulation is done with liquids other than water [38]. When high alcohols are used as coagulants in experimental trials, Lyocell fibers show skin-core morphology. Such fibers have lower strength which is an undesired fiber property. Fink et al. [33] reported a clever two-stage coagulation technique for Lyocell fibers. Higher alcohols are not miscible with water and are lighter than water. The double coagulation bath, therefore, has the higher alcohol on the top layer and water on the bottom. Consequently, a liquid jet slowly coagulates first at the outer jet boundary, followed by fast coagulation in water. As a result, the fiber surface is more porous (less dense), and the core of the fiber is highly dense and

oriented. The two-stage coagulation technique produces fibers with good strength and high fibrillation resistance.

Typical properties of Lyocell fibers are summarized and compared to other cellulose fibers in Table 4.3 Lyocell fibers have outstanding properties. The main advantages of these fibers in comparison to other fibers are much higher dry and wet strengthes but these fibers have the tendency for a high degree of fibrillation as a disadvantage [41].

Table 4.3 Properties of Various Cellulose Fibers (0: Minimal, 6: Maximum degree of fibrillation) [41]

Property	Cotton	Lyocell	Polynosic	Viscose	Cupro
Degree of Fibrillation	2	4-6	3	1	2-3
Dry Tear Strength (cN/tex)	22	42	38	22	20
Wet Tear Strength (cN/tex)	28	36	30	12	10
Strength Ratio (wet/dry)	~1.25	~0.85	~0.70	0.55	0.50
Water Retention (%)	50	65	55-75	90-100	100-120
Average DP	1600-2000 (bleached)	~600	~500	~300	~500

CHAPTER 5. Experimental Procedure

5.1 Materials

A reagent grade anhydrous ethylenediamine ($NH_2CH_2CH_2NH_2$) was obtained from Fisher Scientific, and reagent grade potassium thiocyanate (KSCN) crystals and sodium thiocyanate crystals were obtained from Sigma-Aldrich.

Three cellulose samples including Waco DP 210, AV cellulose (DP 730) and VFC cellulose (DP 450) were used for the experiments of intrinsic viscosity measurement and dissolution process. All three samples were ground to 40 mesh size in a Wiley Mill and dried in a vacuum oven overnight at 60ºC before use. The KSCN was also dried in a vacuum oven overnight at 60ºC before use.

5.2 Intrinsic Viscosity Measurement

VFC cellulose obtained from Buckeye Company and AV cellulose were used for the experiment of intrinsic viscosity measurement. Calculated amount of dried celluloses (0.2g, 0.4g, 0.6g and 0.8g) were weighed out and transferred quantitatively to a suitable glass flask that can be tightly closed by screw cap. 25 ml of distilled water was added to the flask and shook in order to wet out and disperse the cellulose sample. The air from the flask was swept out with a stream of nitrogen. 25 ml of cupriethylenediamine, then, was added, the cap was inserted tightly, and the solution was shaken in a mechanical shaker bath at 25ºC until the cellulose completely dissolved.

After complete dissolution of cellulose in the solution, 10ml of the cellulose solution was transferred by pipette to a viscometer (100, j420) previously placed in the temperature control bath at 25ºC. The solution was left for at least 5 min to reach bath temperature. By applying suction, the solution into the lower line of the viscometer was drawn until top meniscus is a little above the mark above. The efflux time, the time required for the meniscus to pass from upper mark to the mark below, was measured at least three times.

5.3 Dissolution of Cellulose

5.3.1 ED/KSCN and ED/NaSCN Solvent Preparation

KSCN and NaSCN, chemical reagent grade, were used for maximum solubility without further purification except drying overnight in vacuum oven at 60ºC. A known amount of dried salt was placed in a flask with a magnetic stirrer at room temperature, and then 50ml of ethylenediamine was combined with each salt in the flask. After that, the flask was placed on the stirring plate until the salt was completely dissolved. When the salt was completely dissolved in the ethylenediamine, a known weight of salt was added little by little until the solution reached the maximum solubility.

5.3.2 Cellulose/ED/KSCN Solution Preparation

Two different methods were used for dissolution of cellulose. One is rapid temperature cycling technique developed by Cuculo and Hudson. A solution of salt in ED was chilled in a freezer at ca. -20ºC for 15 min. A known weight of cellulose was then combined with cold solvent and placed in a sealed polyethylene bag at ambient temperature. The intermittent shearing was required to increase solubility of cellulose for about 30 min. Several times of temperature cycling were required for complete dissolution of cellulose.

The other method is dissolving cellulose at high temperature (70-80ºC) (Figure 5.3.2.1). A solution of salt in ED was combined with a known weight of cellulose in a three neck flask at room temperature. The flask with the mixture was placed into oil bath and connected with condenser and mechanical stirrer, and cold water kept circulating through the condenser to avoid evaporation of ED. The temperature was then increased up to 70 to 80ºC with the stream of nitrogen gas. It took 5-10 min to reach the temperature 70 - 80ºC.

Complete dissolution of cellulose was confirmed using a polarized light microscope.

Figure 5.1 Experimental Set-up for Cellulose Dissolution Process

5.4 Coagulation Study

5.4.1 Film Formation

Cellulose solution films were formed by spreading solutions on glass plates. Several layers of scotch tape at the edges were used to control the film thickness. Plates with cellulose solutions were immersed in several different coagulants for 30-60 min. The resulting cellulose films were dried at room temperature overnight.

5.4.2 Measurement of Coagulation Rate of Cellulose Solutions

In order to determine the coagulation rate, the cellulose/ED/KSCN (7/65/35) solutions were prepared at high temperature (70ºC). To prepare specimens, a glass capillary tube (1.0 mm diameter, 10 cm length) was used, and the solution was placed in the capillary tube at high temperature (60-70ºC). The measuring apparatus (Figure 5.2) were prepared to determine the diffusion rate of coagulant into the solution. Methanol and water were used in each experiment as coagulants, and fluorescein was added to determine a clear moving boundary in methanol. The moving boundary was observed and boundary distances were recorded with time.

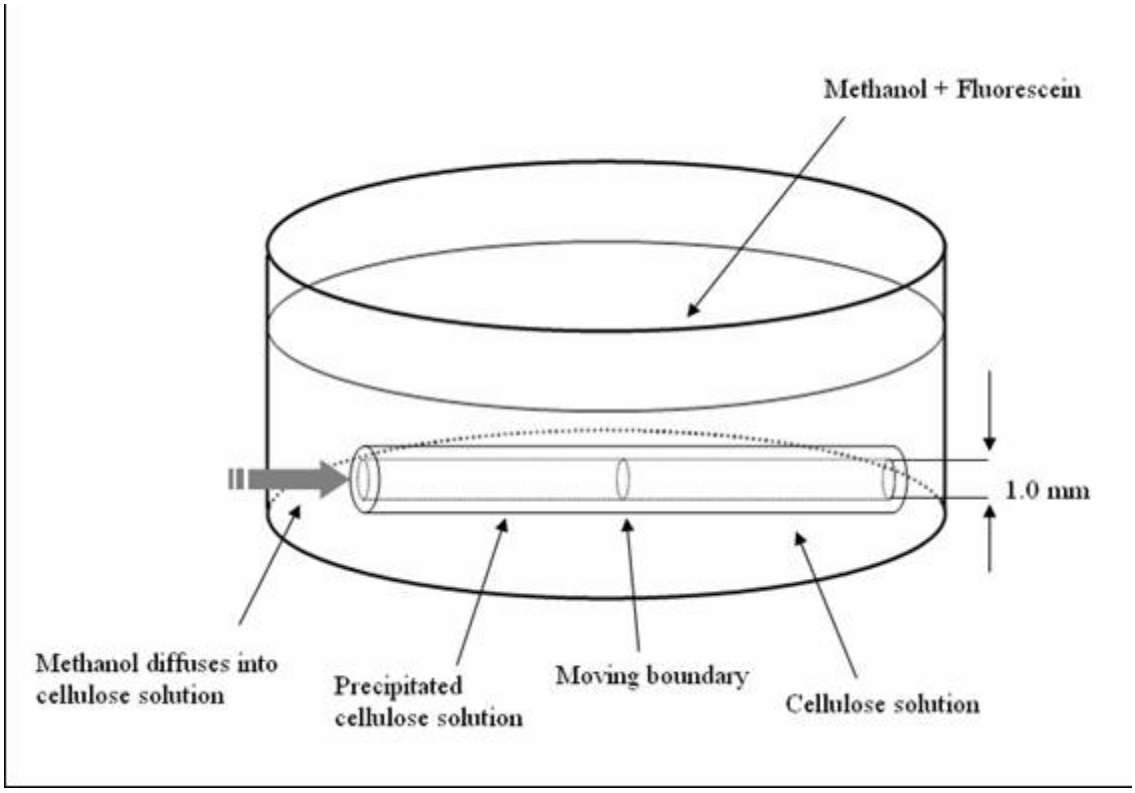

Figure 5.2 Schematic of Coagulation Rate Experiment Set-up

5.5 Dry Jet-Wet Spinning of Cellulose/ED/KSCN Solution

The spinning system consists of a Bradford piston spinning unit, a coagulation bath, one stage drawing section, and a fiber winding. The cellulose solution used in the spinning experiments was the cellulose/ED/KSCN (7/65/35), which has the best spinnability, and it was preheated about 60-70ºC before the spinning. The solution was first forced through a filter and then extruded through a spinneret (3 holes, 80μm hole diameter) into a coagulation bath (1m length) at room temperature. The coagulated filaments were then taken up by the first nip roller and stretched through the second nip roller under room temperature. The

resulting fibers were wound up by a winder. In order to remove the residues in the fibers, the resulting fibers were washed out in the water overnight and dried at room temperature. The extrusion velocity, first and second nip roller speed and final take-up speed were controlled depending on the situation. The immersion length of the filaments in the coagulation bath and length of air gap between extruder and coagulation bath were both set at 10 to 15 cm. Drawn fibers were soaked in the ionized water overnight to remove any traces of ED and KSCN.

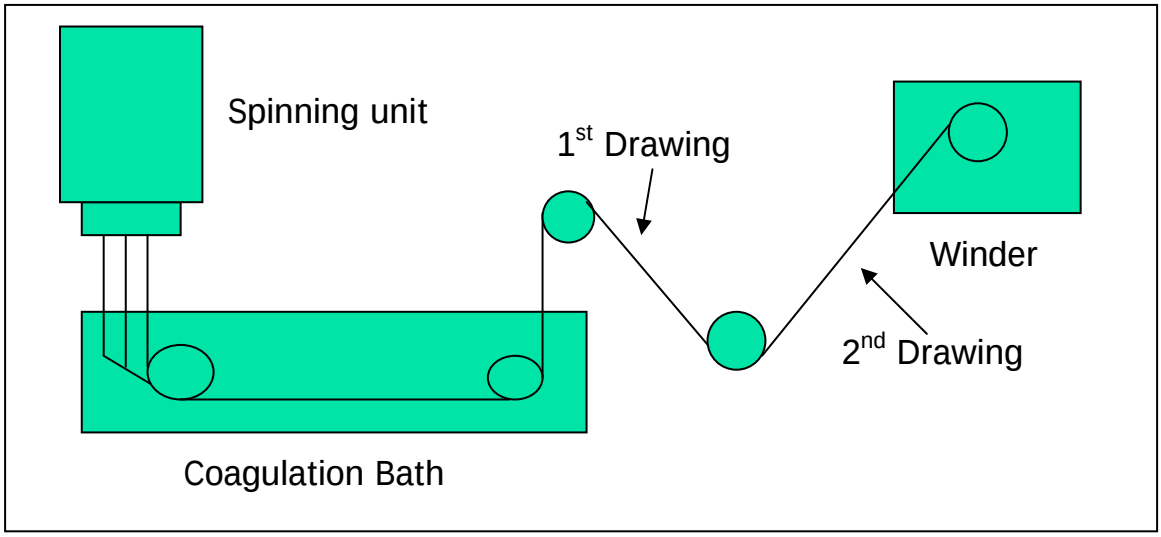

Figure 5.3 Schematic of the Dry Jet-Wet Spinning System of Cellulose Fibers

5.6 Characterization of Cellulose Fibers via ED/KSCN Solvent System

5.6.1 Tensile Properties of Cellulose Fibers

Tensile properties of cellulose fibers produced from cellulose/ED/KSCN (7/65/35) solution were observed. The measurement of tensile properties was referred to ASTM D 3822. Prior to testing, the fibers were conditioned at temperature of 70 ^{o}F and relative humidity of 65% for 24 hours. The measurements were done on single end fiber using 10 samples and 1 inch gage length. Crosshead speed and initial speed of test were both set at 15.0 mm/min. The average denier of each sample was used as an input, and a 5lb load cell was used to measure the tensile properties of the cellulose fibers by a SinTech® tensionmeter.

5.6.2 X-ray Diffraction Analysis

The X-ray scans of cellulose fiber produced from cellulose/ED/KSCN (7/65/35) solution was performed with a Seimens type F X-ray diffractometer. The X-ray source was Ni-filtered Cu Kα radiation (30kV, 20mA). The sample was mounted on aluminum frames and scanned from 5 to 30º (2θ) at a speed of 1.0º/min.

5.6.3 FTIR Spectroscopy Analysis

The resulting cellulose fibers produced from cellulose/ED/KSCN (7/65/35) solution were prepared for FTIR spectroscopy test. FTIR spectra of the cellulose fibers were obtained

using a Nicolet 510P FTIR Spectrophotometer equipped with attenuated total reflectance (ATR).

5.6.4 DSC Analysis

Cellulose fibers via ED/KSCN solvent system and cellulose/ED/KSCN (7/65/35) solution for differential scanning calorimeter (DSC) experiments were prepared to analyze the remaining salt in the fibers. Thermal analysis of cellulose fibers and cellulose/ED/KSCN (7/65/35) solution was conducted on a PerkinElmer Instruments Diamond DSC differential scanning calorimeter. Samples were heated from 25ºC to 300ºC at a rate of 20ºC/min.

CHAPTER 6. Results and Discussion

6.1 Viscosity Measurement

Salt concentration, salt type, cellulose concentration, and cellulose molecular weight all play important roles in the cellulose dissolution process and spinning process [21]. Among them, cellulose molecular weight is largely related to numerous properties of cellulose. These properties are also very important in the fiber formation process and in their effect on the fiber properties. In general, an increase in the molecular weight of cellulose is usually related to increase in tensile strength, toughness, and abrasion resistance. Viscosity of a cellulose solution varies according to concentration and molecular weight of the dissolved cellulose. As molecular weight and concentration increase, the viscosity increases and cellulose has difficulty in dissolution. Therefore, accurate determination of the molecular weight of cellulose is very important for the dissolution of cellulose, the fiber formation process and the resulting fiber properties.

Intrinsic viscosity of VFC cellulose and AV cellulose is measured followed by ASTM 1795 and calculated molecular weight and degree of polymerization of two different celluloses based on the viscosity measurement.

Relative viscosity (η_{rel}) is the ratio of the viscosity of a solution (η) to the viscosity of the solvent used (η_s). If both solution and solvent are measured in the same viscometer, relative viscosity can be obtained directly from the ratio of outflow times:

$$\eta_{rel} = \frac{\eta}{\eta_s} \text{ and/or } \eta_{rel} = \frac{t}{t_0} \qquad (6.1.1)$$

Where:
η_{rel} = relative viscosity
η = viscosity of solution
η_s = viscosity of solvent
t_0 = outflow time of solvent, (s)
t = outflow time of solution, (s)

Specific viscosity (η_{spec}) expresses the incremental viscosity due to the presence of the polymer in the solution. This is also equal to the relative viscosity of the same solution minus one:

$$\eta_{spec} = \frac{\eta - \eta_s}{\eta_s} \text{ and/or } \eta_{spec} = \eta_{rel} - 1 \qquad (6.1.2)$$

The reduced viscosity is the ratio of the specific viscosity to the concentration which indicates the capacity of a polymer to cause the solution viscosity to increase, in other words the incremental viscosity per unit concentration of polymer.

$$\eta_{red} = \frac{\eta_{spec}}{c} \qquad (6.1.3)$$

Like other polymer solution properties, the cellulose solution used for viscosity measurements is not ideal and so reduced viscosity depends on concentration. As with osmotic pressure, it will be useful to extrapolate to zero concentration. The extrapolated value of reduced viscosity at zero concentration is the intrinsic viscosity, ([η]). The intrinsic

viscosity is used as a unique function of molecular weight and measurement of intrinsic viscosity can be used to measure molecular weight.

$$\lim_{c \to 0} \frac{\eta_{spec}}{c} = [\eta] \qquad (6.1.4)$$

The inherent viscosity (η_{inh}) is the ratio of the natural logarithm of the relative viscosity to the concentration of the polymer.

$$\eta_{inh} = \frac{\ln \eta_{rel}}{c} \qquad (6.1.5)$$

Table 6.1 and Table 6.2 show the different viscosities of AV cellulose and VFC cellulose calculated from viscosity measurement. In the case of VFC cellulose, 8 different concentrations are decided to measure the viscosity accurately. As seen in the table, relative viscosity and specific viscosity are gradually increased with the increment of cellulose concentration. The reduced viscosity, the ratio of the specific viscosity to the concentration, is also increased. In contrast, the inherent viscosity is decreased little by little as the cellulose concentration is increased.

Table 6.1 Viscosity Measurement of AV Cellulose

Concentration (wt %)	Average Flow Time of Solution (sec.)	Average Flow Time of Solvent (sec.)	η_{rel}	η_{spec}	η_{red}	η_{inh}
0.0382	95.27	79.9	1.19	0.19	5.03	4.60
0.0604	105.15	79.9	1.32	0.32	5.23	4.55
0.0831	116.19	79.9	1.45	0.45	5.46	4.51
0.1045	127.57	79.9	1.60	0.60	5.71	4.48

Table 6.2 Viscosity Measurement of VFC Cellulose

Concentration (wt %)	Average Flow Time of Solution (sec.)	Average Flow Time of Solvent (sec.)	η_{rel}	η_{spec}	η_{red}	η_{inh}
0.0197	90.43	85.45	1.06	0.06	2.96	2.88
0.0501	98.32	85.45	1.15	0.15	3.01	2.80
0.0792	106.58	85.45	1.25	0.25	3.12	2.79
0.1002	112.30	85.45	1.31	0.31	3.13	2.72
0.2088	149.52	85.45	1.75	0.75	3.59	2.68
0.4133	239.49	85.45	2.80	1.80	4.36	2.49
0.6081	358.25	85.45	4.19	3.19	5.25	2.36
0.7978	508.35	85.45	5.95	4.95	6.20	2.24

Based on the viscosity measurement, the intrinsic viscosities of AV cellulose and VFC cellulose are obtained by plotting the graph (Figure 6.1-2). The extrapolated value of reduced viscosity and inherent viscosity at zero concentration become equal to the intrinsic viscosity (Table 6.3).

Table 6.3 Intrinsic Viscosity of AV Cellulose and VFC Cellulose Calculated From Different Methods

	Intrinsic Viscosity, [η] (dl/g)		
Calculation Method	Reduced Viscosity	Inherent Viscosity	Martin Equation
AV Cellulose	4.63	4.67	4.67
VFC Cellulose	2.77	2.84	2.89

The Mark-Houwink equation describes the dependence of the intrinsic viscosity of a polymer on its relative molecular mass and is expressed:

$$[\eta] = K \cdot M_r^{\alpha} \qquad (6.1.6)$$

where, [η] is the intrinsic viscosity, K and α are constants the values of which depend on the nature of the polymer and solvent as well as on temperature, and M_r is one of the relative molecular mass averages. In the case of natural cellulose, the values of K and α are equal to 0.0000395 and 1. Degree of polymerization, then, can be calculated by dividing the total molecular weight of cellulose into the molecular weight of the repeating unit (Table 6.4).

Table 6.4 Molecular Weight and Degree of Polymerization (DP) of AV Cellulose and VFC Cellulose

	Molecular Weight, (M_w, g/mol)			Degree of Polymerization (DP)		
Calculation Methods	Reduced Viscosity	Inherent Viscosity	Martin Equation	Reduced Viscosity	Inherent Viscosity	Martin Equation
AV Cellulose	117233	118213	118305	724	730	730
VFC Cellulose	70111	72023	73148	433	445	451

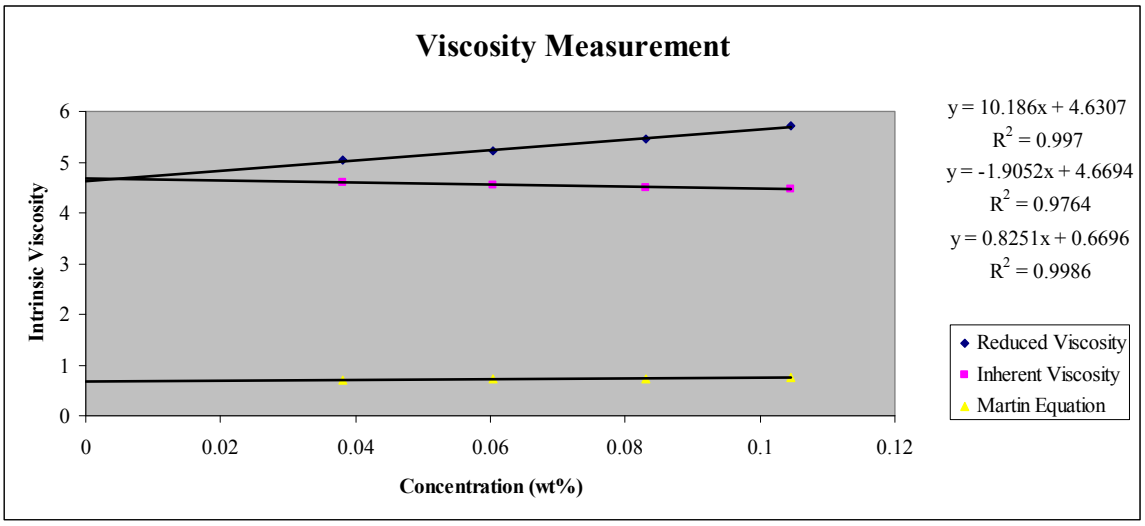

Figure 6.1 Viscosity Measurement of AV Cellulose

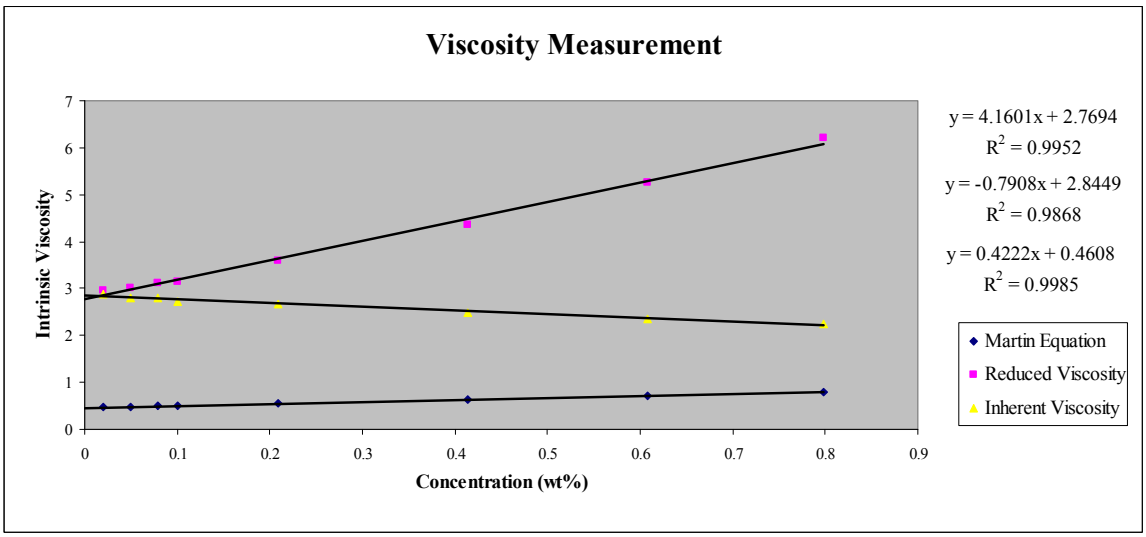

Figure 6.2 Viscosity Measurement of VFC Cellulose

6.2 Solubility of Cellulose in the ED/KSCN and ED/NaSCN Solvent

To figure out the best ratio of ED/KSCN solvent and ED/NaSCN solvent for the dissolution of cellulose, several different ratios of ED/KSCN and ED/NaSCN solvents are prepared and the maximum solubility of KSCN and NaSCN into ED and the maximum solubility of cellulose into the ED/KSCN solvents and the ED/NaSCN solvents are observed. The maximum solubility of KSCN and NaSCN is 44 wt% and 46 wt% at room temperature. These two salts show similar solubility in ED.

Table 6.5 shows the solubility of cellulose in different ratios of ED/salt solvents. VFC cellulose (DP 450) is used for dissolution processes and the concentration of cellulose is 5 wt% for all experiments. The dissolution processes are performed at high temperature (60~70ºC) and also use temperature cycling technique. To compare the cellulose dissolving ability in different ratios of ED/salt solvent under the same conditions, the solvent concentration is expressed (w/w) ED/salt. As seen a Table 6.5, at salt concentration in the range less than 20%, both ED/KSCN and ED/NaSCN solvents do not dissolve cellulose. On the other hand, at salt concentrations in the range of 30-40% using high temperature procedure and 25-35% using temperature cycling technique, cellulose is dissolved very efficiently in ED/KSCN solvent. ED/NaSCN solvent can dissolve cellulose partially in the range of 35-40% of salt concentration, but cannot achieve the complete dissolution of cellulose. Figure 6.3 displays the polarized light microscopy images of 5 wt% VFC cellulose, which is dissolved in several different ratios of ED/KSCN and ED/NaSCN solvents at high temperature. As seen in the images, the image from cellulose dissolved in proper ratio of ED/KSCN solvent is barely observed the undissolved particles (Figure 6.3 (a)). In contrast,

the image from cellulose in ED/NaSCN solvent and ED/KSCN solvent not in the range of 30-40% display plenty of undissolved cellulose particles (Figure 6.3 (b) and (c)). In this study, the ED/KSCN solvent in the salt concentration range of 30~40% shows better dissolving power than ED/NaSCN solvent in any salt concentration ranges. The dissolution process performed at high temperature is also more efficient to achieve the complete dissolution of cellulose and also the high concentration of cellulose solutions.

Table 6.5 Solubility of VFC Cellulose (DP 450) in Different Ratio of ED/salt Solvents: X (No Solution), O (Solution), Δ (Partially Dissolved Solution)

Ratio of ED/Salt	ED/KSCN		ED/NaSCN	
	High Temp.	Temp. Cycling	High Temp.	Temp. Cycling
85/15	X	X	X	X
80/20	X	X	X	X
75/25	X	O	X	X
70/30	O	O	X	X
65/35	O	O	Δ	Δ
60/40	O	X	Δ	Δ
50/50	No Solvent	No Solvent	No Solvent	No Solvent

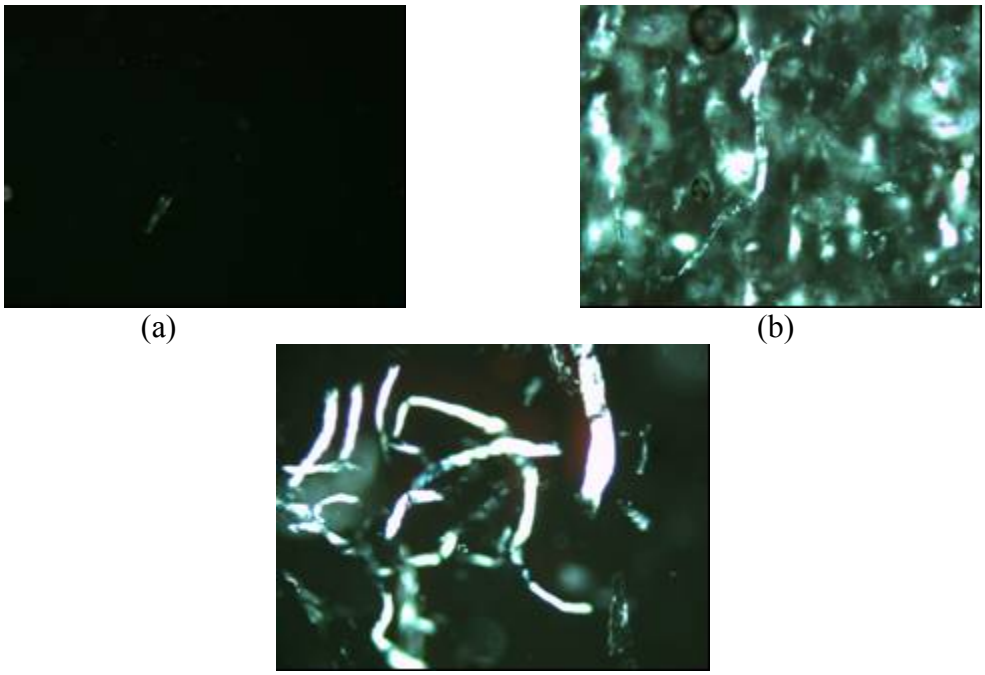

Figure 6.3 Polarized Light Microscopy Images of 5 wt% VFC Cellulose Dissolved in (a) ED/KSCN (65/35), (b) ED/KSCN (85/15), (c) ED/NaSCN (60/40)

6.3 Coagulation Studies

6.3.1 Film Formation

Water, ethanol, methanol, 2-propanol and acetone are tested as possible coagulants by casting films from cellulose/ED/KSCN (7/65/35) solutions (Figure 6.4).

Films coagulated in water show the rapid coagulation rate and turn white in color rapidly. However, the film is relatively brittle and easily breaks. Ethanol and methanol as coagulants produce relatively tougher films and those films are clear and colorless. The coagulation rates of those films are not much different from each other. Although methanol shows a relatively rapid coagulation rate, ethanol takes time to complete the coagulation of film. 2-propanol and acetone are also used to test for possible coagulants. Films coagulated by 2-propanol show good properties in strength and show clear and colorless, but 2-propanol takes too long to coagulate for cellulose films. Acetone, as seen in Figure 6.4 (e), is not effective in removing the ED/KSCN solvent inside of solutions. The remaining solvent causes the films to turn yellowish in color. Acetone seems not to be appropriate for the proper coagulant for cellulose/ED/KSCN solution.

Figure 6.5 shows the SEM images of cellulose films coagulated in water and methanol. The SEM images are taken of the cross-section and surface of cellulose film formed by cellulose/ED/KSCN (7/65/35) solution. The SEM images display different morphologies of cellulose films depending on different coagulants. Films coagulated in water are highly porous in the cross-sectional SEM image and a tough surface is observed. This can be attributed to a rapid diffusion of KSCN and into water. Both compounds are highly

soluble in water. On the other hand, film coagulated in methanol shows much more compact morphology than the one coagulated in water and smooth surface. Solubility of KSCN in methanol is about 20 wt%. No porosities are observed in this film. It can be concluded that methanol provides a mild coagulation rate for cellulose/ED/KSCN solution and it helps the cellulose film form more compact structure and smooth surface.

Table 6.6 Solubility of KSCN in Different Coagulants

Coagulants	Solubility of KSCN (wt%)
Methanol	20
Ethanol	15
2-propanol	5

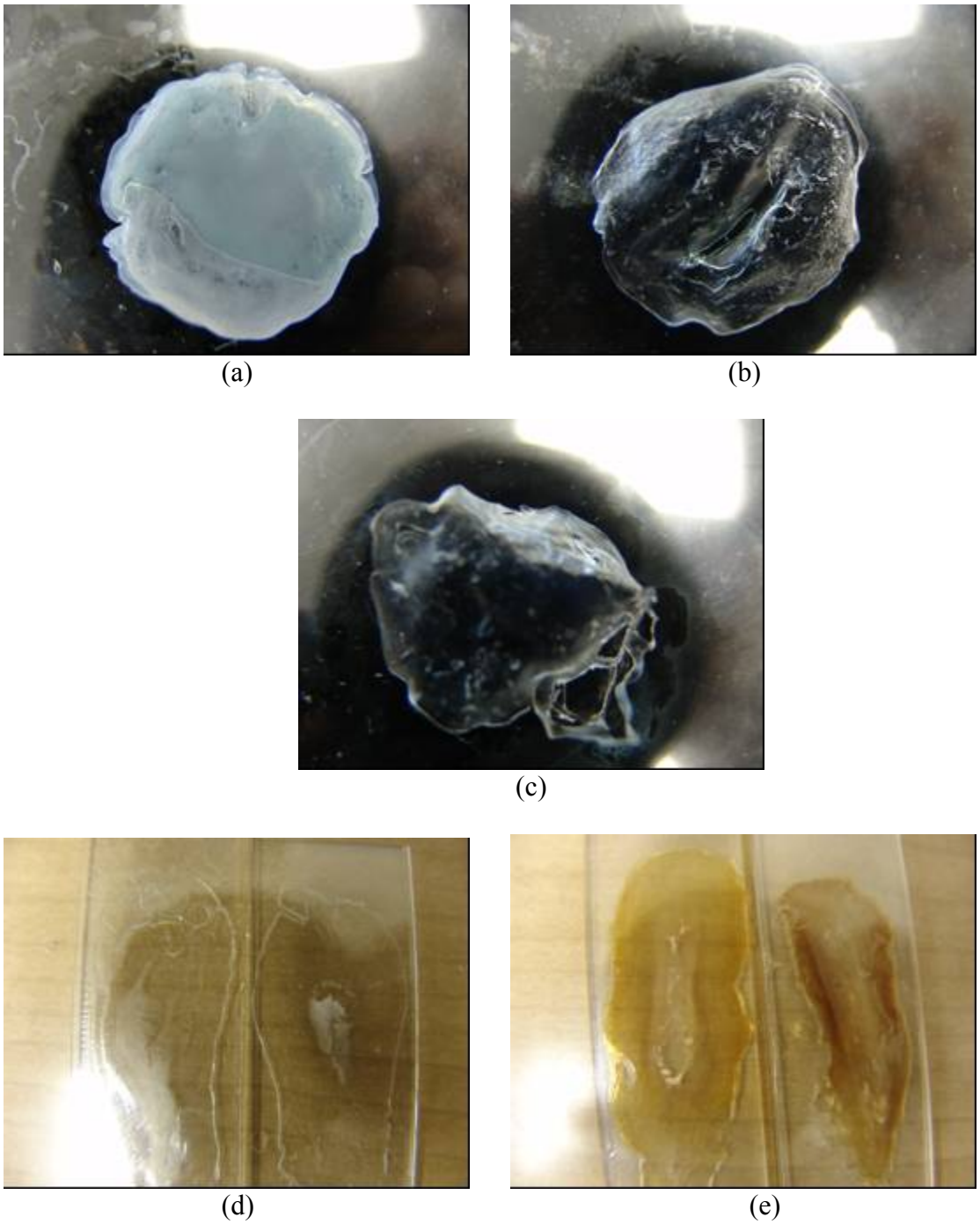

Figure 6.4 Films coagulated in: (a) Water, (b) Ethanol, (c) Methanol, (d) 2-propanol and (e) Acetone

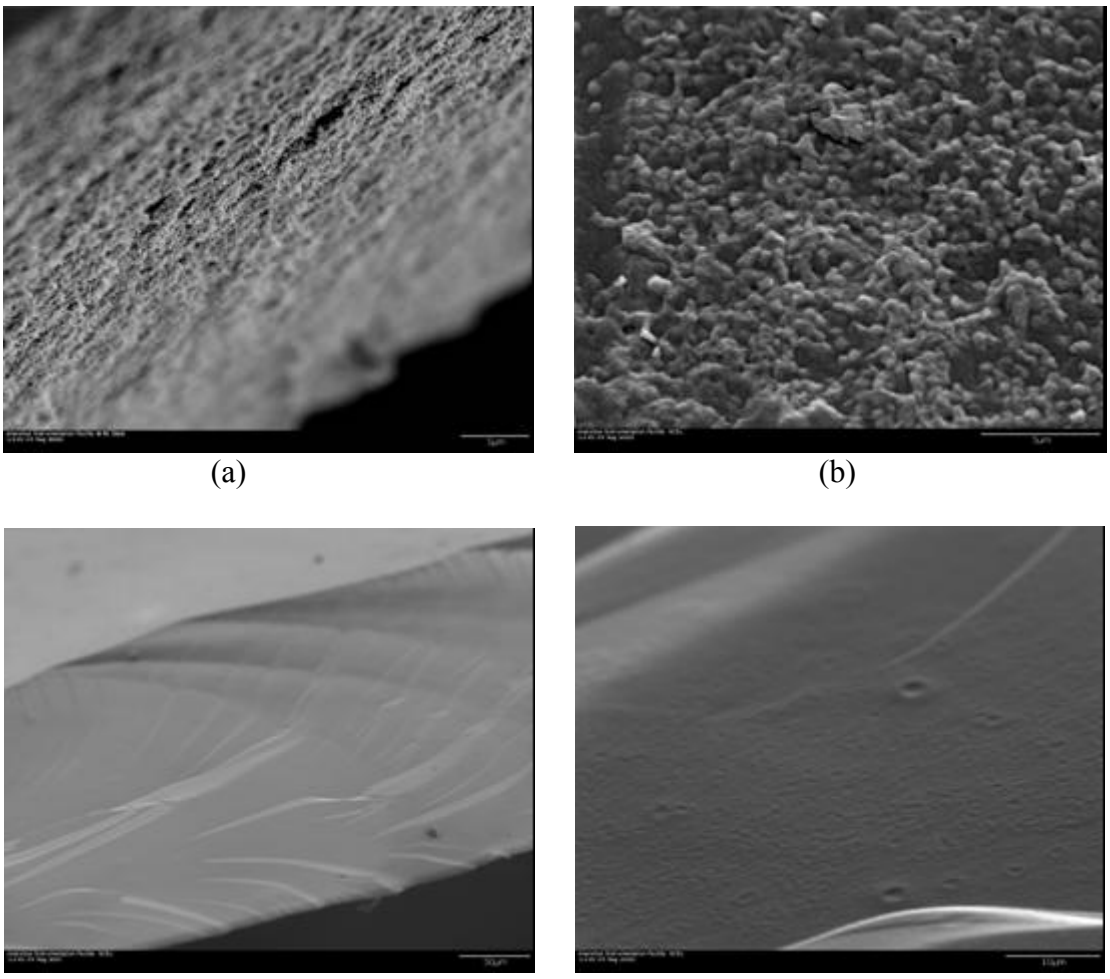

(a) (b)

(c) (d)

Figure 6.5 SEM Images of Cellulose Films Coagulated in Water and Methanol: (a) cross section of cellulose film coagulated in water, (b) surface of the cellulose films coagulated in water, (c) cross section of cellulose film coagulated in methanol and (d) surface of cellulose film coagulated in methanol

6.3.2 Coagulation and Boundary Movement

The boundary movement associated with coagulation is observed for methanol as coagulant. This experiment is performed on a gelled cellulose/ED/KSCN (7/65/35) solution. Figure 6.6 shows the typical data, indicating that the boundary position is proportional to the square root of time in the period of coagulation.

The explanation of the square root of time relationship which appears in the boundary movement is based on Fick's diffusion law [43]. For a linear one-dimensional system, the equation for the diffusion of a coagulant into the cellulose solution can be written as follows [42]:

$$\frac{\partial C_n}{\partial t} = D_n \frac{\partial^2 C}{\partial x^2} \qquad (1)$$

where, C_n and D_n are the concentration and the diffusion coefficients, respectively. The solution of this partial differential equation is well known [43], as shown:

$$C_n(x,t) = A\,erf\left(\frac{x}{2\sqrt{D_n t}}\right) + B \qquad (2)$$

where, A and B are constant of integration, erf( ) is an error function. Since the coagulant concentration at the surface of cellulose solution (x = 0) is constant and equal to $C_{n,0}$, the solution becomes

$$C_n(x,t) = A\,erf\left(\frac{x}{2\sqrt{D_n t}}\right) + C_{n,0} \qquad (3)$$

At the coagulation boundary (x = d), the concentration of coagulant reaches a critical value (C^*_n), which causes the cellulose to precipitate or crystallize from the solution. It follows that

$$A = \frac{C_n^* - C_{n,0}}{erf\left(\frac{x}{2\sqrt{D_n t}}\right)} \qquad (4)$$

It indicates that $d/\sqrt{t}$ should have a constant value. In other words, the boundary position is proportional to the square root of time in the period of coagulation.

In practice, the coagulant used in the fiber spinning process should provide a sufficient coagulation rate to fully coagulate the fiber within a specified time scale. Otherwise, unexpected defects can be caused in the resulting fibers, such as a hollow fiber. The equation for the relationship between the spinning conditions and the minimum coagulation rate is derived from Liu et al. [43].

$$(d/\sqrt{t}) = 0.7(D/2)(v/L)^{1/2} \qquad (5)$$

where, D is the diameter of the spinneret orifice and L and v are the immersion distance and the average velocity, respectively, of spun fiber in the coagulation bath. The spinning conditions used in the formation of cellulose fibers are plugged into the equation (5) to confirm the complete coagulation of resulting fibers. The minimum coagulation rate ($d/\sqrt{t}$) is calculated from the slope of graph in Figure 6.6 and the real coagulation rate is calculated from the equation (5) as plugged in the experimental spinning conditions:

D = the diameter of the spinneret orifice = 0.08 mm

L = the immersion distance = 100 cm

v = the average velocity of spun fibers in the coagulation bath = 35.3 m/min

The calculated minimum coagulation rate is 1.66×10^{-1} mm/min$^{1/2}$ and the real coagulation rate for methanol is obtained as 3.75×10^{-1} mm/min$^{1/2}$. As a result, the real

coagulation rate for methanol is good enough for providing a sufficient coagulation rate to fully coagulate the spun fibers in our spinning system. Table 6.7 displays the comparison of coagulation rate of each coagulant versus minimum coagulation rate for our spinning system. Based on the experiment, the methanol is the only coagulant to provide efficient coagulation time to the cellulose fibers, because the coagulation rates for other coagulants do not exceed the minimum coagulation rate for our spinning system

.

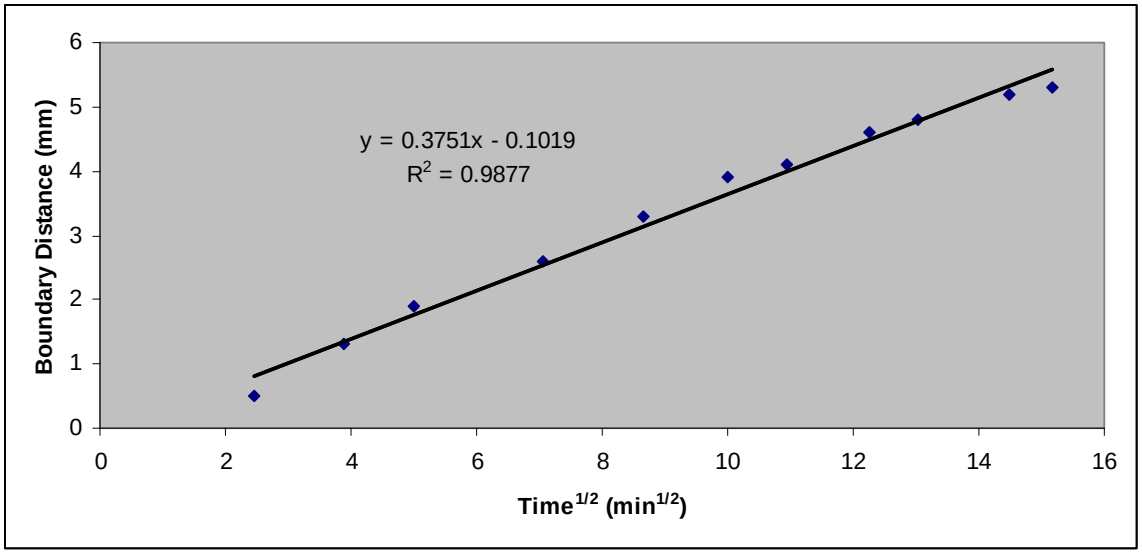

Figure 6.6 Boundary Movement in the Coagulation Process of Cellulose/ED/KSCN (7/65/35) Solution

Table 6.7 Comparison of Coagulation Rate of Each Coagulant vs. Min. Coagulation Rate

Coagulant	Coagulation Rate, ($mm/min^{1/2}$)		Min. Coagulation Rate, ($mm/min^{1/2}$)
Methanol	3.751×10^{-1}	>	1.66×10^{-1}
Ethanol	9.129×10^{-2}	<	1.66×10^{-1}
2-Propanol	4.564×10^{-2}	<	1.66×10^{-1}
tertiary-butanol	1.862×10^{-2}	<	1.66×10^{-1}

6.3.3 Diffusion Coefficient

The diffusion coefficient of methanol into cellulose/ED/KSCN (7/65/35) solution is calculated through the Stoke-Einstein equation;

$$D = \frac{K_B \cdot T}{6 \cdot \pi \cdot \eta \cdot R_0} \qquad (1)$$

,where D is the diffusion coefficient, K_B is Boltzman's constant ($1.381 \times 10^{-23} JK^{-1}$), T is temperature, η is viscosity of medium and R_0 is radius of the solute molecule. This equation can be applied to a small and rigid sphere solute diffusing into a solvent [44]. Liu et al. [43] and Knaul et al. [45] developed an equation to examine the reliability of the Stroke-Einstein equation for the coagulant and polymer solution system;

$$\ln \frac{d^2}{t} = A - \frac{B}{3} \ln V \qquad (2)$$

,where d is the boundary distance, t is time, V is the molecular volume of the coagulant and A and B are adjustable constants. When the straight line relationship is seen in a plot of ln d^2/t versus ln V for several coagulants with different molecular volumes, the Stoke-Einstein equation can be applied for the diffusion coefficient. Several different coagulants are observed to confirm the applicability of the Stoke-Einstein equation of the cellulose/ED/KSCN (7/65/35) solution and methanol system. Table 6.8 displays experimental values of boundary distance of cellulose/ED/KSCN (7/65/35) solution with several different coagulants for 120 min and the experimental values are plotted in Figure 6.7. The graph shows the linear relationship of ln d^2/t and ln V. The linear relationship between ln

d^2/t and ln V indicates the molecular volume dependence of the coagulation rates. The linear regression equation relating methanol, ethanol, 2-propanol and tertiary-butanol is shown:

$$\ln \frac{d^2}{t} = 19.89 - 7.01 \ln V \qquad (3)$$

Since the several coagulants with different molecular volume shows linear relationship with cellulose/ED/KSCN (7/65/35) solution, the diffusion coefficient can be calculated from the Stoke-Einstein equation. Figure 6.8 indicates the viscosity of cellulose/ED/KSCN (7/65/35) solution at 60ºC depending on the shear stress. The cellulose solution shows Newtonian behavior in the shear stress range of 0 to 100 Pa and the viscosity at zero shear stress obtained from the graph is 36.82 Pa.s. The radius of methanol (2.5×10^{-8} cm) can be calculated from the molecular volume of methanol with the assumption that the methanol is a spherical molecule. The calculated diffusion coefficient of methanol into cellulose/ED/KSCN (7/65/35) solution is 2.65×10^{-8} cm^2/sec.

Table 6.8 Experimental Values of Boundary Distance of Cellulose/ED/KSCN (7/65/35) Solution with Several Coagulants for 120 minutes

Coagulant	Molecular Volume, (cm^3/mol)	Boundary Distance, (mm)	ln V	ln d^2/t
Methanol	40.4	4.3	3.699	-5.965
Ethanol	58.4	1	4.067	-8.881
2-Propanol	76.2	0.5	4.333	-10.268
Tertiary-butanol	94.9	0.2	4.553	-12.101

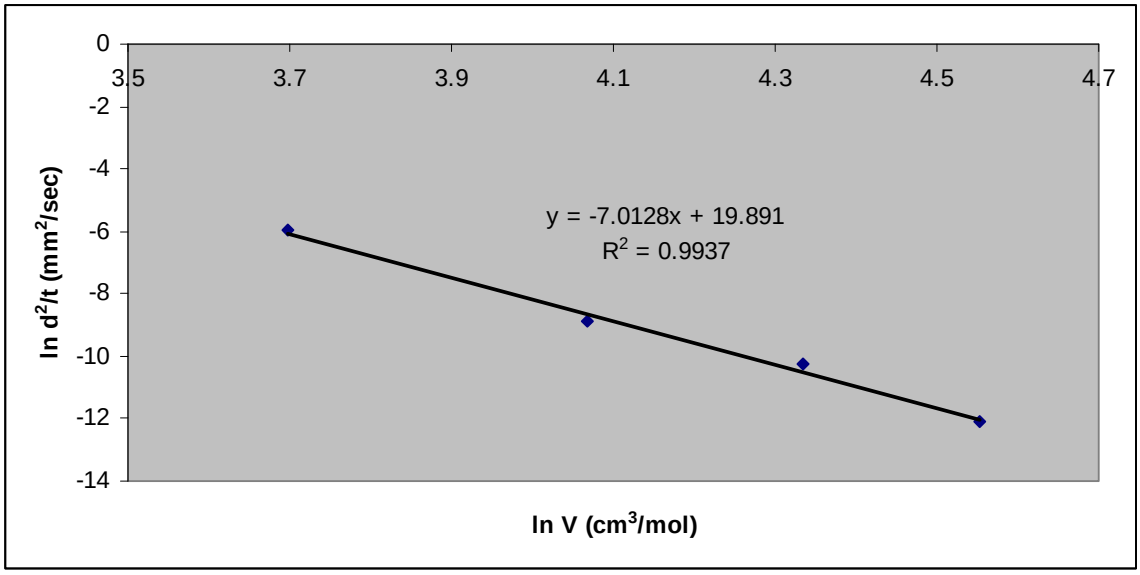

Figure 6.7 Dependence of coagulation rate at 120 min on the molecular volume of the coagulants for cellulose/ED/KSCN (7/65/35)

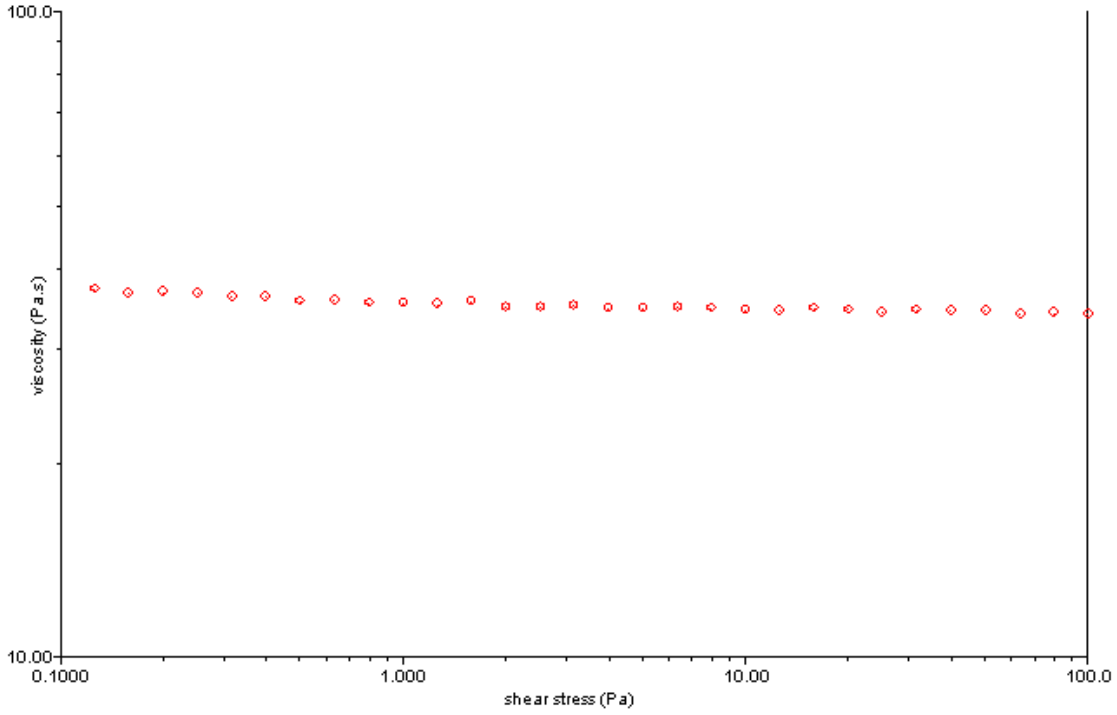

Figure 6.8 Viscosity of Cellulose/ED/KSCN (7/65/35) Solution at 60ºC

6.4. Dry Jet-Wet Spinning of the Cellulose/ED/KSCN Solutions

A 7 wt% of cellulose ED/KSCN solution has been found to be an excellent spinning dope for celluloses with DP greater than 400.

Since ionic liquids have recently been reported to dissolve cellulose, 1-butyl-3-methylimidazolium was also used for comparison. Interestingly, at the same polymer concentration (DP = 450) the ED/KSCN spinning dope is a free flowing viscous solution, but the solution produced from the ionic liquid is a highly viscose solution, which is not appropriate for the wet spinning. Figure 6.9 displays the comparison of cellulose solutions produced from the ED/KSCN and the ionic liquid solvent system.

So the cellulose fibers via the ED/KSCN solvent system are successfully spun by the dry-jet wet spinning method. Table 6.9 shows the typical spinning conditions of dry jet-wet spinning in the ED/KSCN solvent system. The temperature of the cellulose/ED/KSCN (7/65/35) solution is adjusted to 60-70ºC by using a heating tape and 125μm spinneret with a single hole is used in the study. It is based on my observation that, while performing the spinning procedure, the solution is continuously comes out from the hole of spinneret and the spinning conditions are stable and consistent. The resulting fibers are also uniform and show the good physical properties, relatively. However, the average linear density of resulting fibers is somewhat higher when compared to the fibers used for the textile applications. The typical commercial cellulose fibers have a denier in the range from 3 to 7.

In order to produce lower denier fibers, three round hole spinnerets having diameter of 50 and 80μm are also used for the spinning process. Although the cellulose fibers are well produced and collected on the bobbin with a new type of spinneret, the spinning process

shows a significant instability. The cellulose solution is not extruded continuously from the three holes of spinneret. Usually, the solution comes out from a single hole out of three holes and one filament is collected and drawn through the spinning system. Several trials were performed to adjust this problem. Namely, we lowered the concentration of cellulose solution to reduce the viscosity and increased the spinneret size to reduce the shear stress. However, both approaches did not fully correct the problem. The similar problem has occurred in our lab with other polymer solutions and could be related to undissolved polymer particles. However, no undissolved cellulose particles were found in our polymer solutions.

It is based on my assumption that one of the possible reasons for the unstable spinning condition is uneven pressure distribution in the barrel that is caused by decreasing the amount of polymer solution during spinning. An uneven pressure distribution could lead to uneven extrusion through the three holes of spinneret. The other possible reasons can be solution viscosity fluctuations and the unevenly distributed temperature in the spinning pack and the spinneret. These reasons can bring out the one or two holes of spinneret to be blocked, because of the gelation of cellulose solution and cause the spinning condition to be unstable.

I believe that the unstable spinning conditions appeared when we used the small diameter size with the three hole spinneret. This effect can be easily corrected by using a single screw extruder equipped with a metering pump. A metering pump can adjust the flow rates of solution which are precise when averaged over the spinning time. Since the extruder is also equipped with heating zones, a uniform heating should eliminate viscosity fluctuations and should lead to uniform extrusion.

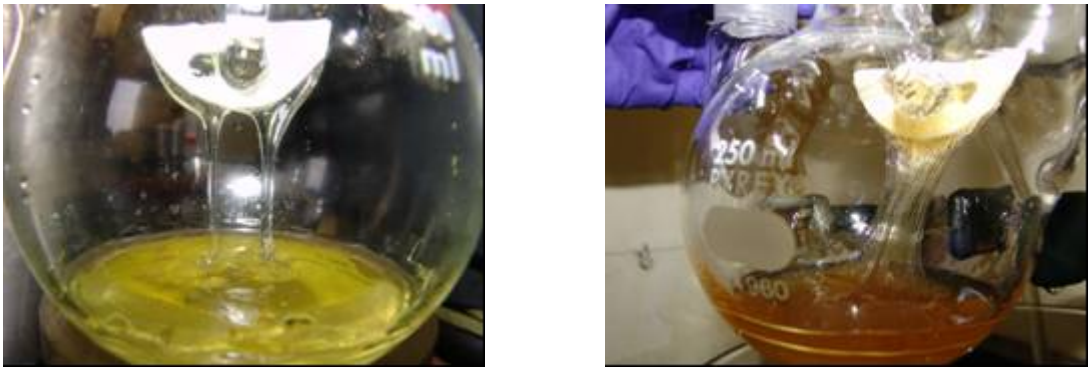

(a) (b)

Figure 6.9 Viscosity Comparison for: a) Free Flowing Fiber Forming Cellulose/ED/KSCN (7/65/35) Solution b) Non-fiber Forming Highly Viscous Solution of Cellulose in 1-butyl-3-methylimidazolium chloride (ionic liquid). C = 7% w/w; DP = 450.

Table 6.9 Typical Spinning Conditions of the Dry Jet-Wet Spinning in the ED/KSCN Solvent System

Air Gap (cm)	15	Spinning Temp. (ºC)	60-70
Orifice Diameter (μm)	125	Drawing Speed (m/min)	35.3
Shape	Round	Draw Ratio	2.5
L/D Ratio	2.5	Coagulation Liquid	Methanol
Piston Speed (mm/min)	1.5	Coagulation Temperature	Ambient Temperature

6.5 Characterization of Cellulose Fibers via ED/KSCN Solvent System

6.5.1 Mechanical Properties of Cellulose Fibers via ED/KSCN Solvent

Cellulose fibers via ED/KSCN solvent system are successfully produced by a dry jet-wet spinning system. For the characterization of cellulose fibers spun by ED/KSCN solvent system, VFC cellulose/ED/KSCN (7/65/35) solution was used. In the dry jet-wet spinning process, there are plenty of variables which can affect the mechanical properties of fibers, such as spinning temperature, spin draw ratio, air gap distance, and drying conditions of the fibers. In our spinning system, spin draw ratio affects the mechanical properties of fibers most than any other variables. Table 6.10 shows different mechanical properties of cellulose fibers depending on the denier and spin draw ratio. As decreasing the denier of cellulose fibers, the fiber tenacity and fiber modulus tend to increase gradually. In contrast, the fiber elongation decreases with an increasing spin draw ratio. The elongation value on the 15 denier fiber is based on the assumption that the fibers do not stand the load cell weight due to their brittleness. Table 6.11 shows the comparison of mechanical properties of commercial cellulose fibers and cellulose fibers via the ED/KSCN solvent system. Hyosung and Lenzing cellulose fibers are produced by the NMMO solvent system and are used for tire cord and textile applications. When compared to those three cellulose fibers, our cellulose fibers show potential possibilities to reach commercial values after further research.

Table 6.10 Mechanical Properties of Cellulose Fibers via ED/KSCN Solvent

Denier	Draw Ratio	Fiber Modulus, (gf/denier)	Fiber Tenacity, (gf/denier)	Elongation, (%)
11	3.5	153.84	3.63 ± 0.32	15.41
13	2.5	137.16	3.07 ± 0.21	27.49
15	1.5	134.5	2.24 ± 0.28	12.64

Table 6.11 Mechanical Properties of Commercial Cellulose Fibers vs. Cellulose Fibers via ED/KSCN Solvent System

	Denier	Tenacity, (gf/denier)	Elongation, (%)
Hyosung, (Lyocell)	1500	7.00	6.5
Lenzing Fibers	6.0	4.18	13
ED/KSCN Solvent	11	3.63	15.41

6.5.2 Scanning Electron Microscopy (SEM) Analysis

The surface and fractured cross sectional SEM images of cellulose fibers spun by the cellulose/ED/KSCN (7/65/35) solution are shown in Figure 6.10. Figure 6.10 (a) is the cross-sectional SEM image of a cellulose fiber drawn at room temperature. Unlike viscose rayon, the fiber shows a round shape and a relatively compact structure on their morphology. Although Lyocell fibers generally show their micro-fibrils as a disadvantage on the fractured cross section of fibers, the micro-fibrils are not observed for this fiber. Figure 6.10 (b) is also the cross-sectional SEM image of a cellulose fiber drawn at a hot temperature (100ºC). The fiber also shows round shape like the fiber drawn at room temperature, but the morphology displays a more compact structure. As a result, the fibers drawn at a hot temperature show a higher tensile strength than the fibers drawn at room temperature. Figure 6.10 (c) is the surface of the cellulose fiber. This image shows the smooth surface and no fibrillation.

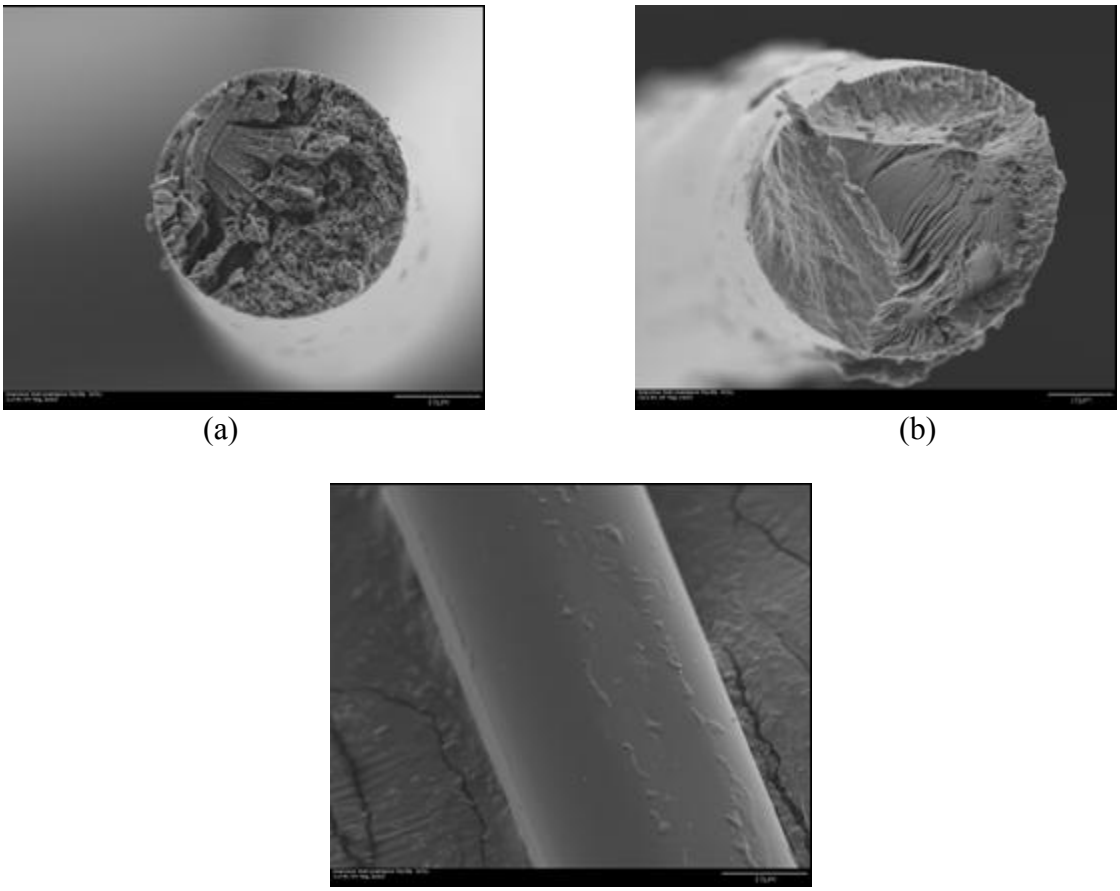

(a) (b)

(c)

Figure 6.10 SEM Images of Cellulose Fibers Produced via ED/KSCN Solvent system: (a) Cross-section of cellulose fibers with cold drawing, (b) Cross-section of cellulose fibers with hot drawing, (c) Surface of cellulose fibers

6.5.3 FTIR and DSC Analysis of Cellulose Fibers

FTIR and DSC analysis of cellulose fibers are performed to analyze the remaining salt content in the cellulose fibers spun by the ED/KSCN solvent system. Figure 6.11 shows FTIR spectra of VFC cellulose pulp and cellulose fibers spun by the ED/KSCN solvent system. The FTIR spectrum shows almost the same peaks with cellulose pulp and cellulose fibers. The peak characteristics of C≡N group in thiocyanates generally shows the range of 2130-2190 cm^{-1}, but any peaks in the range are not observed in the spectrum of cellulose fibers. The absence of a peak at 2130-2190 cm^{-1} characteristic of the SCN group of KSCN in the FTIR spectrum indicates that there is no residual salt in the cellulose fibers via the ED/KSCN solvent system. In other words, our coagulation and washing fiber with water is effective in removing KSCN from the cellulose fibers via the ED/KSCN solvent system. The FTIR analysis also suggests that the cellulose fibers are not in a derivative form since no new absorption peaks appears in the spectra.

DSC analysis is also used to figure out the remaining salt in the cellulose fibers. Figure 6.12 indicates the DSC thermogram of the cellulose/ED/KSCN (7/65/35) solution and cellulose fibers via the ED/KSCN solvent system. The cellulose solution in the thermogram shows the peak at 180ºC, the melting point of KSCN, but cellulose fibers do not have any peak in that range. The absence of a peak at 180ºC in the DSC thermogram of cellulose fibers also indicates that there are no residual KSCN in the cellulose fibers.

FTIR and DSC analysis confirms the cellulose fiber via the ED/KSCN solvent system does not have the remaining salt.

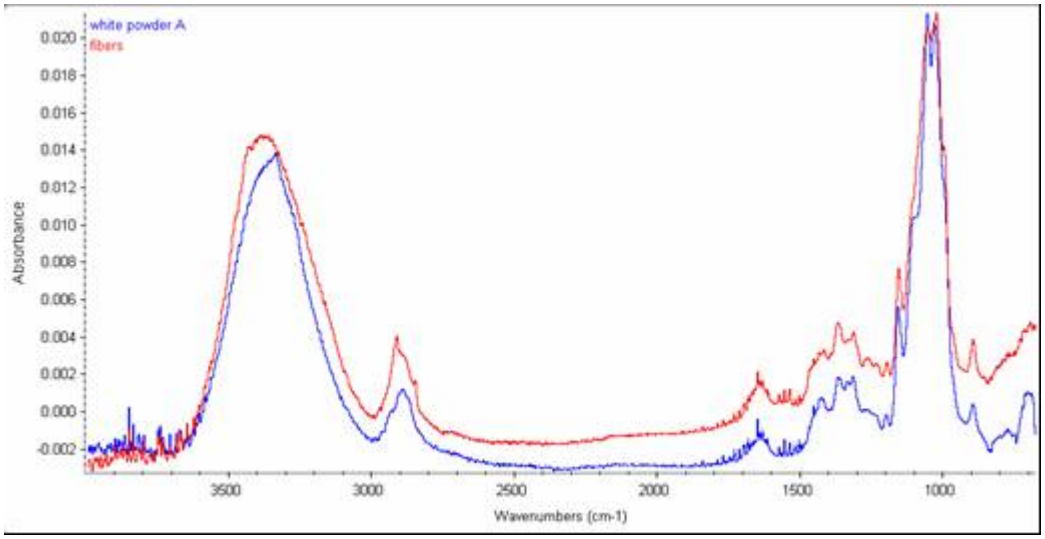

Figure 6.11 FTIR Spectra of VFC Cellulose Pulp and Cellulose fibers spun by ED/KSCN Solvent System.

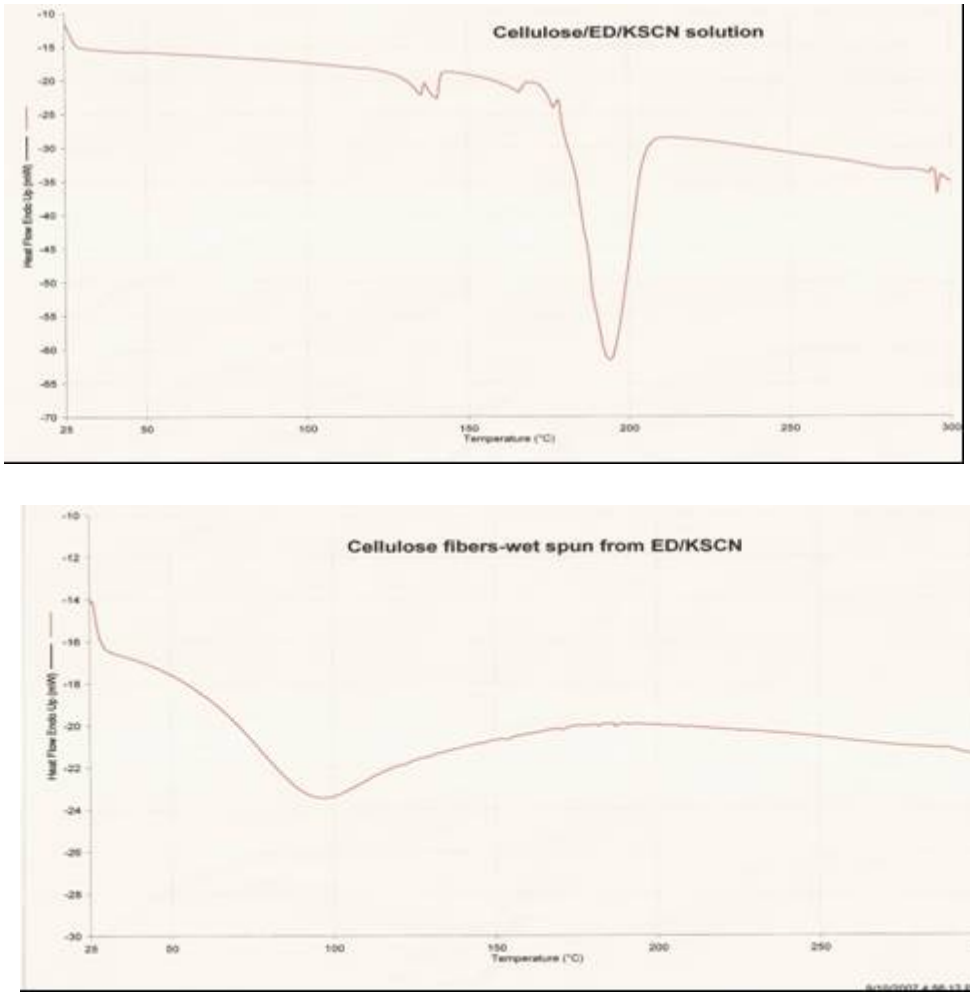

Figure 6.12 DSC Thermogram of Cellulose/ED/KSCN (7/65/35) Solution and Cellulose Fibers via ED/KSCN Solvent system

CHAPTER 7. Conclusion

Cellulose is considered to be one of the most abundant nature polymers worldwide as well as a biodegradable and renewable polymer. Despite lots of advantages regarding end use of cellulose, there is a need for a multiple solvents system and a large amount of time to achieve cellulose dissolution. In addition, by products and side reaction in the cellulose dissolving process have significant negative environmental and health effects that are cost ineffective. This study introduced one excellent solvent system that is combined with ethylenediamine (ED) and potassium thiocyanate (KSCN) in a certain ratio. This solvent system was simple and direct as well as inexpensive and environmentally friendly when compared to current solvent systems.

In the ED/KSCN solvent system, salt type, salt concentration, cellulose concentration and cellulose molecular weight were important factors in the dissolution of cellulose as well as the formation of fibers. Polarized light microscopy images showed that ED/KSCN solvent in the range of 30-40% exhibits the best dissolving ability for cellulose when compared to the ED/NaSCN solvent system. The ED/KSCN solvent could dissolve the VFC cellulose (DP 450) concentration up to 12 wt% and AV cellulose (DP 730) concentration up to 10 wt%. However, 7 wt% of VFC cellulose concentration had the best spinnability for the spinning process.

In the coagulation studies, the boundary movement of cellulose/ED/KSCN (7/65/35) solution was directly proportional to the square root of time for each coagulant tested. The coagulation rate measurement also showed that the most significant variable affecting the

coagulation process of the cellulose/ED/KSCN solution is the nature of the coagulant. The molecular sizes play an important role in determining the rate of coagulation. Of all the coagulation studies, methanol was found to be the most effective coagulant for cellulose/ED/KSCN solutions. The minimum coagulation rate and diffusion coefficient for cellulose/ED/KSCN (7/65/35) were also calculated by the equation derived by Liu and Cuculo et al. The minimum coagulation rate calculated for the present spinning system is 1.66×10^{-1} mm/min$^{1/2}$ and the diffusion coefficient of methanol into cellulose/ED/KSCN (7/65/35) solution is 2.65×10^{-8} cm^2/sec. Methanol as a coagulant was the only useful coagulant with our spinning system.

The cellulose fibers via the ED/KSCN solvent system were characterized by the mechanical property test, SEM analysis, FTIR and DSC analysis. In our spinning system, the spin draw ratio affected the mechanical properties of cellulose fibers the most. As the spin draw ratio increases, the fiber tenacity and fiber modulus tend to increase gradually but fiber elongation decreases. For the morphology test of cellulose fibers via the ED/KSCN solvent system, unlike viscose rayon, the fiber showed round a shape and a relatively compact structure, and the micro-fibrils generally observed at Lyocell fibers were not observed. The cellulose fibers drawn at a hot temperature (100ºC) showed more compact structure than the fiber drawn at room temperature and showed higher tensile strength. FTIR and DSC analysis revealed that the cellulose fibers via the ED/KSCN solvent system have no remaining salt. This is confirmed by no observations of the peak characteristic of C≡N group in thiocyanate in FTIR analysis and no observations of the melting point (180ºC) of KSCN in DSC analysis.

CHAPTER 8. Future Work

The method of preparing the cellulose/ED/KSCN (7/65/35) solution has been established at the high temperature (60-70 ºC) and by the temperature cycling technique. The rheological characterization of solution prepared at the high temperature has shown the reversible viscosity dependence on the temperature changes. The solution at the high temperature is a free flowing viscous solution, but if it stays at room temperature for a while, the solution turns into a highly viscous gel. However, the solution prepared by the temperature cycling technique does not show any viscosity changes at room temperature. Investigation of the extensional viscosity of solutions depending on the temperature changes and the different methods may be useful. This would allow one to establish the extensional flow behavior of the solution with various temperature ranges and the result may be used to optimize the best temperature ranges for the spinning process.

The spinning of the cellulose solutions was done using methanol as a coagulant at room temperature. The use of different coagulants with different temperature for the spinning has been used in the technical literature to produce improved fiber properties. Investigation of other possible coagulants using single or multiple components with various temperature ranges may be useful to further improve the fiber properties as well as to demonstrate the effectiveness of this cellulose-solvent system as the logical choice for alternate and viable processing to other cellulose-solvent system. One possible coagulant of multiple components is the mixture of ethanol and water. Ethanol is relatively less toxic and environmentally friendly than methanol and shows good properties as coagulant for our solvent system, but,

as a disadvantage, has low coagulation rate for our spinning system. On the other hand, water as a coagulant produces relatively brittle cellulose films but shows the very rapid coagulation rate. We expect that if water is added to ethanol, the mixture could increase the coagulation rate for the spinning system and produce good properties of cellulose fibers.

Our research work demonstrated that spinning of cellulose/ED/KSCN solution can produce cellulose fibers with good mechanical properties. We also showed the use of a piston type spinning machine is not very useful to produce multiple filament low denier cellulose yarns. Further spinning work should include a single screw extruder equipped with a metering pump and a smaller hole spinneret to assure good temperature distribution. This spinning should include the use of multiple-hole spinneret, which should provide enough filaments for further study in dyeing and fabric formation of this cellulose fiber.

References

1. Kristen Carranco, Margaret Frey, Cellulose Fiber Spinning, (http://matdl.org/repository/eserv.php?pid=matdl:405&dsID=n2004_CCMR_REU_Carranco.pdf)

2. T. P. Nevell, S. H. Zeronian, Cellulose Chmistry and Its Applications, 1985

3. Margaret W. Frey, Hester Chan, Kristen Carranco, Rheology of Cellulose/KSCN/Ethylenediamine Solutions and Coagulation into Filaments and Films, Wiley InterScience (www.interscience.wiley.com), (2005)

4. V. Tripp and C. Conrad, Chapter 5 X-ray Diffraction, Instrumental Analysis of Cotton Cellulose and Modified Cotton Cellulose, Edited by R. O'Corner, Marcel Dekker Inc., New York, 1972.

5. Usa Sangwatanaroj, The Mechanism of Dissolution of Cellulose in the Ammonia/Ammonium Thiocyanate Solvent, M. Sc. Thesis, North Carolina State University, NC

6. Richard Kotek, Handbook of Fiber Chemistry 3rd Edition, Regenerated Cellulose Fibers, Chapter 10, 667-771

7. F. A Bujitenhuis, M Abbas, A. J. Witteveen, The degradation of and Stabilization of Cellulose Dissolved in N-Methylmorpholine-N-oxide (NMMO), Papier 40, 615-619 (1986)

8. H. Lang, I. Laskowski, B. Lukanoff, H. Schleicher, H. Mertel, H. Franz, E. Taeger, Untersuchungen an Losungen von Cellulose in N-Methylmorpholine-N-oxide (NMMO), Cell. Chem. Technol. 20, 289-301 (1986)

9. E. Taeger, H. Franz, H. Mertel, Probleme der schwefelkohlenstofffreien Verformung von Zellulose zu textilen Zellulosefaden mittels N-Methylmorpholin-N-oxides, Formeln, Faserstoffe, Fertigware 4, 14-22 (1985)

10. T. Rosenau, A. Potthast, H. Sixta, P. Kosma, The Chemistry of Side Reactions and Byproduct Formation in the System NMMO/Cellulose (Lyocell Process), Progr. Polym. Sci. 26 (9), 1763-1873 (2001).

11. Chanzy H., Nawrot S., Peguy A., and Smith P., J. Polym. Sci., Polym. Phys. Ed., 1982, 20, 1909.

12. Thomas Rosenau, Tom Elder, Antje Potthat, Herbert Sixta and Paul Kosma, The Lyocell Process: Cellulose Solution in N-Methylmorpholine-N-oxide (NMMO) – Degradation Processes and Stabilizers, 12th International Symposium on Wood and Pulping Chemistry, June 9-12, Madison, Wisconsin, p. 305-308.

13. Dawsey T.R. and McCormick C.L. 1990, The Lithium Chloride/Dimethylacetamide Solvent for Cellulose: Literature Review. J. Macromol. Sci. – Rev. Macromol. Chem. Phys. C30: 405 -440

14. Anne-Laurence Dupont, Cellulose in Lithiun Chloride/N,N-Dimetylacetamide, Optimisation of a Dissolution Method Using Paper Substrates and Stability of the Solutions, Polymer 44 (2003) 4117-4126

15. Shengdong Zhu, Yuanxin Wu, Qiming Chen, Ziniu Yu, Cunwen Wang, Shiwei Jin, Yigang Ding and Gang Wu, Dissolution of Cellulose with Ionic Liguids and Its Application: a mini-review, The Royal Society of Chemistry 2006, Green Chem., 2006, 8, 325-327.

16. Hudson, S.M and Cuculo, J.A., J. Polym. Chem. Ed., 1982, 20, 499

17. De Groot, A.W., Carroll, F.I., and Cuculo, J.A., J. Polym. Sci., Polym. Chem. Ed., 1986, 24, 673.

18. J.A. Cuculo, C. B. Smith, U. Sangwatanaroj, E. O. Stejskal, and S. S. Sankar, A study on the Mechanism of Dissolution of the Cellulose/NH_3/NH_4SCN System II, J. Polym. Chem. Vol. 32, 241-247 (1994)

19. Cuculo, J. A., B. Smith, et al, A Study on the mechanism of dissolution of the cellulose/NH_3NH_4SCN system I, J. Polym. Chem. Vol. 32, 229 (1994)

20. Hattori K, Abe E et al., New solvent for cellulose II.; Ethylenediamine/thiocyanate salt system, Polym. J. 36(2), 123-130

21. Min Xiao, Margaret W. Frey, The role salt on cellulose dissolution in ethylenediamine/salt solvent systems, Springer Sci., Vol. 14, 225-234 (2007)

22. Margaret W. Frey, Lei Li, Min Xiao and Troy Gould, Dissolution of Cellulose in Ethylenediamine/salt Solvent System, Springer Netherlands, Vol. 13, 147-155 (2006)

23. Brendler E., Fisher S. and Leipner H., Li NMR as Probe for Solvent-Cellulose Interactions in Cellulose Dissolution, Cellulose 8, 283-288 (2001)

24. Oh SY, Yoo DI et al., Crystalline Structure Analysis of Cellulose Treated with Sodium Hydroxide and Carbon Dioxide by Means of X-ray Diffraction and FTIR Spectroscopy, Carbohydrate Res 340(15), 2376-2391 (2005)

25. Nwlson ML, O'Connor RT, Relation of Certain Infrared Bands to Cellulose Crystallinity and Crystal Lattice Type I. Spectra of Lattice Type I, II, III and of Amorphous Cellulose, J. App. Polym. Sci. Vol. 8 (3), 1311-1324 (1964)

26. Cadars S, Lesage A et al., Chemical Shift Correlations in Disordered Solids, J. Am. Chem. Soc., Vol. 127(12), 4466-4476

27. Nehls I, Wagenknecht W et al., Characterization of Cellulose and Cellulose Derivative in Solution by High-Resolution C-13-NMR Spectroscopy, Prog. Polym. Sci., Vol. 19(1), 29-78

28. Isogai A, Usuda M et al., Solid-State CP/MAS C-13 NMR Study of Cellulose Polymorphs, Macromolecules, Vol. 22(7), 3168-3172 (1989)

29. Bochek AM, Effect of Hydrogen Bonding on Cellulose Solubility in Aqueous and Nonaqueous Solvents, Russ. J. Appl. Chem., Vol. 76(11), 1711-1719 (2003)

30. Henrissat B., Marchessault RH et al., A Solid-State C-13 NMR Study of the Cellulose I-Ethylenediamine Complex, Polymer Communications, Vol. 28(4), 113-115 (1987)

31. Numata Y, Kono H et al., Cross-Polarization/Magic Angle Spinning C-13 Nuclear Magnetic Resonance Study of Cellulose I-Ethylenediamine Complex, J. Biosci. Bioeng., Vol. 96(5), 461-466 (2003)

32. Horii F, Hirai A et al., Solid-State C-13 NMR Study of Conformation of Oligosaccharides and Cellulose – Conformation of CH_2OH Group about the Exo-Cyclic C-C Bond, Polymer Bull., Vol. 10(7-8), 357-361 (1983)

33. Fink, H. P., Weigel, P., Purz, H. J., and Ganster, J., Prog. Polym. Sci., Vol. 26, 1473 (2001)

34. Laszkiewicz, B., Manufacture of Cellulose Fibers without the Use of Carbon Disulfide, ACGM LODART, SA, Lodz, Poland (1997)

35. Rosenau, T., Potthast, A., Sixta, H., and Kosma, P., Prog. Polym. Sci., Vol. 26, 1763, (2001)

36. Maia, E., Peguy, A., and Perez, S., Acta Crystallogr., Sect. B: Struct. Crystallogr. Cryst. Chem., Vol. 37(10), 1858 (1981)

37. Wachsman, U., and Diamantoglou, M., Das Papier, Vol. 51(12), 660 (1997)

38. Fink, H. P., Purz, H. J., and Weigel, P., Das Papier, Vol. 51, 643 (1997)

39. Mortimer, S. A., and Peguy, A. A., Cellulose Chem. Technol., Vol. 30, 117 (1996)

40. D. B. Kim, J. J. Pak, S. M. Jo, W. S. Lee, Dry Jet-Wet Spinning of Cellulose/N-Methylmorpholine N-Oxide Hydrate Solutions and Physical Properties of Lyocell Fibers, Textile Res. J., Vol. 75(4), 331-341 (2005)

41. Breier, R., Lenzinger Berichte, Vol. 76, 108 (1997)

42. J. Crank, The mathematics of Diffusion, Oxford University Press, London (1975)

43. C. K. Liu, J. Cuculo, B. Smith, Coagulation Studies for Cellulose in the Amonia/Amonium Thiocyanate (NH_3/NH_4SCN) Direct Solvent System, J. Polym. Sci.: Polym. Phy., Vol. 27, 2493-2511 (1989)

44. S. W., Ha, Structural Study of Bombyx Mori Silk Fibroin during Processing For Regeneration, PhD Dissertation, North Carolina State University, Raleigh, (2004)

45. J. Z. Knaul, K. A. M. Creber, Coagulation Rate Studies of Spinnable Chitosan Solutions, J. Appl. Polym. Sci., Vol. 66, 117-127 (1997)

46. K. Hattori, T. Yoshida, J. Cuculo, Dissolution of Cellulose in the Amine/Thiocyanate Salt System